Mineralogical Composition and Origin of Airborne Dust in an Alpine Environment of Hochtor (Hohe Tauern, Austria): Effects on Pedogenesis, Biological Soil Crusts, and Vascular Plant Growth

Thomas Peer[1]*, Ling-Juan Zheng[1], Franz Neubauer[2], Gertrude Friedl[2], Christoph Hauzenberger[3] and Anne Kasper-Giebl[4]

[1]Department of Biosciences, Paris-Lodron University of Salzburg, Salzburg, Austria, [2]Department of Geography and Geology, Paris-Lodron University of Salzburg, Salzburg, Austria, [3]Institute of Earth Sciences, University of Graz, Graz, Austria, [4]Institute of Chemical Technologies and Analytics, Vienna University of Technology, Wien, Austria

There is considerable evidence that mineral dust has an important impact on alpine ecosystems, but the relationship remains unclear in some instances. In an attempt to fill this knowledge gap, we investigated 1) the mineralogical composition of dust components at Hochtor (Hohe Tauern, Austria), 2) its effects on soil formation and biological soil crusts (BSCs), and 3) the effect of mineral dust on plant growth in this interdisciplinary study. Mineral particles such as silicates, carbonates, oxides, volcanic quartz phenocrysts, opaque ore minerals, and spheres, such as microtektites, micrometeorites and fly ash aggregates, were detected using a scanning electron microscope (SEM) equipped with an energy dispersive X-ray spectrometer (SEM-EDX). Rare micrometeorites are of extra-terrestrial origin (cosmic dust) and the decorated spheres are aggregates of fly ashes from anthropogenic origin. In terms of size, fine particles (<100 μm) and coarse particles (>100 μm) characterize the dust composition, originating mainly from adjacent rock outcrops, while the transport from the North African desert appears to be less important and diluted by local sources. The research was carried out as part of the pan-European biodiversity project "Soil Crust International" (SCIN). The results suggest that mineral dust aids in the rapid formation of BSCs in highly disturbed treated plots, and thus, both fine sand and available phosphorus are statistically proven to be determinants of the rapid growth of biocrusts. The number of plant individuals also increases between 2016 and 2020, however at a relatively moderate rate due to permanent mechanical erosion and debris flow within the treatment plots. Silica dust is believed to be a contributing factor to the widespread distribution of silicate plants in limestone habitats, such as *Primula minima* and *Cerastium uniflorum*, two "acidophilic" species that have been tested more closely. Finally, it is deduced that 1) aeolian dust plays a role in the continuous process of soil and crust formation, and 2) it works as a growth regulator in

complex biological communities such as BSCs and vascular plant communities by creating new habitats and increasing biodiversity.

INTRODUCTION

Mineral dust is considered an important component of the atmosphere, geosphere, hydrosphere, and biosphere and is essential for nutrient cycling in soil and ecosystems (Simonson, 1995; Stuut et al., 2009; Muhs et al., 2014; Kanakidou et al., 2018, and references therein). Dust is a complex mixture of inorganic and organic solid particles, which vary in size, shape, chemical composition, physical properties, and origin. Dust is also associated with microorganisms (including pathogens), man-made components (such as synthetic fibres), and other air pollutants (Kellogg and Griffin, 2006; Meola et al., 2015; Maki et al., 2019). During the transportation, dust can interact with local air-borne dust and pollutants, and has a significant impact on the environment.

One of the best-known sites for short-distance transport of aeolian dust in Europe is the "Gamsgrube" above the Pasterze glacier (Austria), where carbon-rich dust particles are removed from the surrounding calcareous slate slopes and their accumulation above silicate bedrock affects both pedogenesis and plant composition (Friedel, 1936; Burger and Franz, 1969). In the Northern Calcareous Alps, the transport of siliceous airborne particles, such as from the siliciclastic basement of the Austrian Eastern Alps, alters soil characteristics through brunification and loamification (Solar, 1964; Biermayer and Rehfuess, 1985; Küfmann, 2003; Küfmann, 2008a; Küfmann, 2008b; Duffy, 2011). Moreover, several studies reported that the transport of Saharan dust to the Alps is considered an important chemical and physical reagent in alpine ecosystems (Haeberli, 1978; Prodi and Fea, 1978; De Angelisi and Gaudichet, 1991; Tomadin et al., 1996; Wagenbach et al., 1996; Coen et al., 2003; Greilinger et al., 2018; Telloli et al., 2018). Saharan dust events were also studied on snowpacks at the high-alpine site of Jungfraujoch (Swiss Alps) by Schwikowsky et al. (1995), on glaciers in the French Alps by Maupetit and Delmas (1994), on the glaciers of Piz Zupò (Swiss Alps) by Sodemann et al. (2005), and on snowpacks in Torgnon, Aosta Valley (Italy) by Di Mauro et al. (2019). Most research has focused on the mineral and elemental composition of the dust, using backward trajectories to calculate the main potential source region of Saharan dust (Middleton and Goudie, 2002; Ansmann et al., 2003; Meola et al., 2015; Greilinger et al., 2018). However, the proportion of Saharan dust must be carefully assessed. Considering the 50% reduction in alpine glacier area between 1850 and 2000 (Zemp et al., 2006), local wind systems (mountain winds) transport large amounts of fine-grained material (alpine loess) from the new foreland each year. All particles are deposited on the ground, and particles from different sources are mixed together.

Previously, Hochtor research was integrated into the pan-European research network BiodivERsA and the SCIN ("Soil Crust International") project, to better understand biological soil crusts (BSCs) across Europe (Büdel et al., 2014). Knowledge about BSC is now very extensive, as shown by numerous publications and articles in edited volumes, like those of Belnap and Lange (2003) and Weber et al. (2016). However, the effect of dust on the forming effect of BSCs has been neglected so far and thus is considered a new topic. There is also the question of whether dust has a negative or positive effect on vascular plants. Both are possible: If the stomata become clogged, the dust can impair the plant's metabolism, and finally they will die. The abrasive force of dust can also damage plants, especially in strong winds. Yan et al. (2011), on the other hand, reported that plants on semiarid grasslands in northern China provide a barrier to wind and soil erosion, enabling areas with higher vegetation cover to extract more nutrients from airborne dust. Rizzolo et al. (2016) investigated mineral nutrients in Saharan dust and their beneficial effects on the Amazon rainforest ecosystem. In our approach, we investigated the role of mineral dust in regulating soil and crust formation and on vegetation in alpine environments. Therefore, we propose the following research objectives: 1) to identify grains transported over short and long distances, 2) to identify their mineralogical and chemical composition, 3) to study effects on soil and BSC formation, and 4) to determine the impact of dust on alpine vegetation. In particular, we studied silicate plants growing on limestone substrates.

MATERIALS AND METHODS

Study Area

The study area is located to the east of Hochtor (2,505 m asl), the highest point of the Grossglockner High Alpine Route, a historical transition and trade route. A wide karst plateau covers an area of about 2.5 km^2, including the so-called "Plattenkar" (47º05′09″ to 47º04′55″N and 12º50′44″ to 12º50′52″E) (Fink, 1984) (**Figure 1**). The study area represents a unique site due to its high elevation (2,550–2,580 m asl) and harsh climate conditions (mean annual temperature of 1.5°C, annual precipitation rate of 1.750–2.000 mm, 270–300 days of snow cover, permafrost, and strong winds caused by convective weather conditions on the alpine chain). The wind direction is mainly southwest, with speeds of 15–20 m/s (Auer et al., 2002). All rocks within the Hohe Tauern are metamorphosed, medium-grained, with mineral grain sizes of 1–2 mm, and highly diverse in terms of the lithological composition (Schmid et al., 2013). In particular, the Hochtor area belongs to the Seidlwinkl Triassic, which is assigned to the Upper Schieferhülle Unit within the Penninic Zone of the Tauern Window (Frank, 1969; Schmid et al., 2013). The local rocks consist mainly of rauwake, a holey, porous cellular limestone marble due to the dissolution of embedded gypsum during ablation. The associated
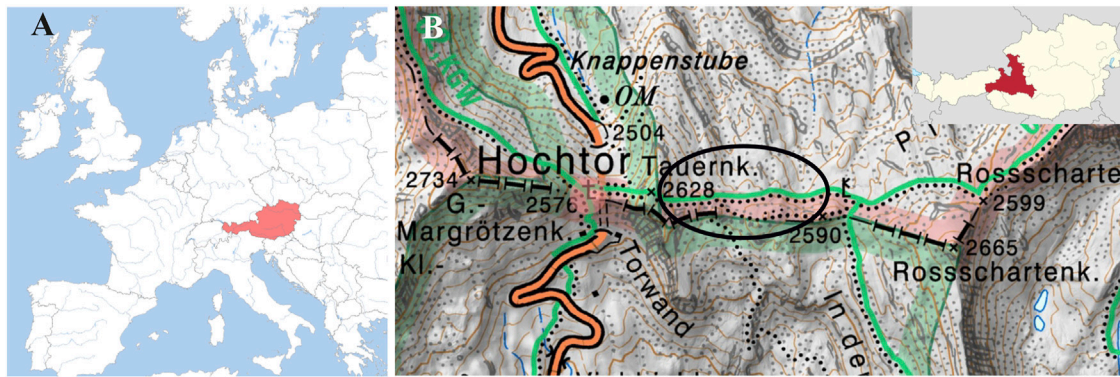
FIGURE 1 | Location of the study. **(A)** Geographical position of Austria (red) within Europe. (https://commons.wikimedia.org/wiki/File:Austria_in_Europe.svg, scale 1: 29.000.000). **(B)** Study area near the Hochtor on the Grossglockner high alpine route (bergfex.at, Austrian map 1:50.000, black oval outline, scale 1:10.000). Top right: Austria and Province Salzburg (red) (File: Salzburg in Austria.svg., scale 1: 13.000.000).

rocks are dolomite and also massive limestone marble. West of Hochtor, Bündnerschiefer of the Brennkogel facies type overlays the Triassic rocks. Dark phyllites and mica-schists (often with garnet) occur frequently; greenschists are subordinate. To the east, the residual hills (monadnocks) of Rossköpfl and Rossschartenkopf are composed of phyllite, mica schists, amphibolite, serpentinite, and quartzite. Many rock constituent minerals from these rocks were found in the deposited dust samples on the Hochtor. Gruber (1980) studied the dust particle deposition in the Glockner area (Hohe Tauern) and reported the average dust particle deposition on snow cover to be 25.3 g/m^2/yr (Hochtor-Sud), 41.5 g/m^2/yr (Hochtor-Nord), and 141.5 g/m^2/yr (Edelweiss peak). Higher values were recorded by deflameters (which collect dust particles carried by the wind), with an average dust particle deposition of 137.6 g/m^2/yr in Hochtor-Sud and 125.9 g/m^2/yr in Hochtor-Nord. The transported and deposited quantity of dust varied significantly from year to year, depending on the specific meteorological situation. Gruber's research indicated grain size ranges from 2 to 50 μm, with a maximum of 200 μm. Muscovite, dolomite, feldspar, quartz, calcite, chlorite, and talc determined the mineralogical composition, most of which originated from adjacent rock outcrops. Significant amounts of CaCO$_3$ in dust samples were also detected, and all deposits caused a calculated soil accretion of 0.01–1.45 mm/yr. Compared with other sites, such as Colle Gnifetti (Swiss Alps), with 0.4–1 g/m^2/yr (Wagenbach and Geis, 1989); southwestern Greenland, with 14.6–65.7 g/m^2/yr (Van-Soest, 2021); and the Mediterranean, with 10–20 g/m^2/yr (Loye-Pilot et al., 1986; Guerzoni et al., 1997), the high amount of deposited dust at the Hochtor may be explained by the strong involvement of local bedrock dust.

Sampling Procedures and Laboratory Analysis

Within the karstified Plattenkar, 10 treatment plots of 100 cm × 100 cm in area were set as part of the BSC project (Büdel et al., 2014). Vegetation was removed from the plots (removal of the upper 1–4 cm thick layer) to examine the successional pattern of recovery, including soil development, plant colonization, and BSC development. Soil samples were collected from treatments (bare soil and new crust) and undisturbed soils (subsoil and topsoil) in 2012, 2014, and 2020. On average, 5–10 samples were collected per plot. The so-called "new crust" was gently scraped from the subsurface along with potentially airborne deposits. In 2020, seven additional samples were collected, five from treatments and two from undisturbed controls. Ten dust-laden snow samples from different sites (approximately 5 m^2 in area) were stored in 1 L plastic bottles and cooled during transportation. Chemical analyses of the soil samples followed the standard methods specified by Zheng et al. (2014). Analyses included the determination of pH, electrical conductivity (EC), total nitrogen (TN), total organic carbon (TOC), available K, Na, Ca, Mg, and P (aK, aNa, aCa, aMg, and aP), and the proportions of sand, fine silt, coarse silt, and clay. In addition, the bioavailability of Fe and Mn in Ethylene Diamine Tetraacetic Acid (EDTA), cation exchange capacity (CEC), and the proportion of exchangeable cations, such as Ca, Mg, K, Al, Fe, and Mn were analysed in 2020 by Austrian Agency for Health and Food Security (AGES) in Vienna. Snow samples were filtered through filters with a pore size of 0.1–10 μm, and the elements Ca, Mg, K, Fe, Al, and P were analyzed in the Salzburg University laboratories using methods conforming to the "International Organization for Standardization" (ISO) and "Deutsches Institut für Normung" (DIN). The resettled higher plants were recorded between July 2016 and July 2020. The thickness of the biological soil crust was measured on a 2 cm thick soil block of 2 cm × 2 cm using a digital caliper (0.01–150 mm) after shaking off the loose material. Ten repetitions were performed; however, very rocky or severely eroded plots were not suitable for this procedure. Extensive statistical analysis was performed on the nine selected soil variables to determine the main factors affecting the growth of biological soil crusts. Statistical analyses were conducted using the Excel XLSTAT software package. Dust samples for mineralogical analysis were collected from 23 different sites in July 2012, 2014, and September 2014. Seven samples (A–G) from dusty snowpacks, six samples (H–M) from cushion plants, and ten samples (N–W) from treatment/restoration plots were collected after all vegetation had

TABLE 1 | Mineralogical composition of the dust samples at the Hochtor, structured by the substrate. A more detailed description of types can be found in the text. Minerals that could not be clearly identified, were question-marked.

No	Substrate	Location	Minerals
A	Snow dust	Plattenkar-Nord 1	Dolomite, quartz, muscovite, decorated sphere, micrometeorite, and etched quartz grains
B	Snow dust	Plattenkar-Nord 2	Dolomite, quartz, magnetite, opaque ore mineral, mica flakes, and Fe-oxide (magnetite?)
C	Snow dust	Plattenkar Sud 1	Quartz, anorthite, muscovite, calcite, and clay minerals
D	Snow dust	Plattenkar Sud 2	Dolomite, muscovite, quartz with dissolution surface, quartz encrusted by limonite, etched quartz, mica flakes, and clay minerals
E	Snow dust	Hochtor 1	Opaque mineral, feldspar, micrometeorite sphere, mica flakes, anorthite, Fe-oxide - magnetite (?), few rounded pitted quartz grains, in part with a limonite crust, and clay minerals
F	Snow dust	Hochtor 2	Calcite, other carbonates (dolomite?), and quartz
G	Snow dust	Edelweiss peak	Fine-grained porous aggregate and cementation by carbonate
H	Plant dust	Way east Hochtor 1	Etched quartz grain, magnetite or hematite, dolomite, amphibole, cementation by carbonate, mica flakes, and few bronze-colored decorated spheres (both >100 µm and <100 µm)
I	Plant dust	Way east Hochtor 2	Dolomite, Fe-oxide (magnetite?), amphibole, few rounded pitted quartz grains; few bronze-colored decorated spheres (>100 µm), clay minerals
J	Plant dust	Hochtor 3	Etched quartz grain, muscovite, few rounded pitted quartz grains, and clay minerals
K	Plant dust	Hochtor Sud 4	Dolomite, rare angular quartz; few rounded pitted quartz grains, and clay minerals
L	Plant dust	Hochtor Sud 5	Dolomite
M	Plant dust	Hochtor Sud 6	Silicate 1, silicate 2, amphibole, opaque ore mineral, Fe-oxide—magnetite (?); few rounded pitted quartz grains
N	Treatment plot	New "crus" 1	Muscovite, quartz, few coated quartz grains
O	Treatment plot	New "crust" 3	Quartz, among them few coated, rounded grains; muscovite, and quartz, clay minerals
P	Treatment plot	New "crust" 5	Dolomite and quartz
Q	Treatment plot	New "crust" 7	Decorated sphere with a recrystallized fine-grained surface
R	Treatment plot	New "crust" 9	Cementation of carbonate
S	Treatment plot	Soil after disturbance plot 1	Heavily disturbed and intergrown by organic material
T	Treatment plot	Soil after disturbance plot 3	Heavily disturbed and intergrown by organic material
U	Treatment plot	Soil after disturbance plot 5	Dolomite
V	Treatment plot	Soil after disturbance plot 7	Quartz, decorated spheres (including a black sphere)
W	Treatment plot	Soil after disturbance plot 9	Dolomite, quartz, and muscovite

been removed. Both <100 µm and >100 µm fractions were analyzed using a scanning electron microscope (SEM, type 100 µm Leica 430). All samples were first examined under a light microscope, and then bulk samples and selected grains were imaged, and the elemental composition was analyzed semi-quantitatively by energy-dispersive X-ray spectroscopy (EDX, type Röntec). A peculiar type of sphere was then investigated using the new JEOL JXA-8230 energy-dispersive spectroscopy (EDS) system equipped with semiquantitative EDX systems at the University of Graz, Austria. Since April 2013, airborne dust particles were regularly measured at the Sonnblick Observatory (3,106 m asl), which is located at a distance of approx. 10 km from the study area at Hochtor. The occurrence of airborne mineral dust originating from long-range transport of desert dust was determined based on its optical properties, i.e., the wavelength dependence of the single scattering albedo (Coen et al., 2003; Schauer et al., 2016).

RESULTS

Mineral Grain Characteristics, Rare Minerals, SEM Images, and Energy-Dispersive Spectroscopy Analyses

The qualitative mineralogical compositions of the 23 dust samples are listed in **Table 1**.

Representative minerals imaged using SEM are shown in **Figure 2**. The focus is on distinguishing external and exotic mineral particles from distant and local sources, assuming that all particles are transported by air. Note that the imaged particles were quite large (the maximum size is given in the description) and had obvious surface characteristics. The separation of individual particles is often difficult because fine-grained samples are typically cemented together with carbonate. For example, the cementation of the aggregates probably occurred during or after deposition under wet conditions on glaciers, and they were then blown away from the glacier foreland (Letsch, 2014). Carbonate can be identified by a set of well-developed cleavage surfaces, and a few mica flakes can be easily identified by their smooth surface (**Figure 2A**). Examination of the overview samples showed that carbonates dominated all the samples. Exotic minerals are unique to the alpine area, which were found in snow patches, plants, and to a lesser extent in treatments, and all were described for the first time in this study (**Figures 2B–F**):

1) Volcanic quartz phenocrysts: In a few rare cases, single crystals of bipyramidal quartz with etched surfaces were observed, with a pyramidal end, but no well-developed prism (**Figure 2B**). On the surface of the prism, traces of etching with small ridges, mostly oriented in parallel, were found, which looked like a printed pattern in micrometer size (**Figure 2B**).

2) Smooth spheres (interpreted as micrometeorites): A peculiar but rare component was represented by a perfect sphere with a smooth surface (**Figure 2C**). These peculiar grains had diameters ranging from 300 to 350 µm. Minerals were not discernible on the surface. The EDX analysis showed that Si, Al, Ca, O, Fe, Mg, and Na (in descending order of abundance) were the major elements, representing an intermediate or mafic melt composition. Unfortunately, a few grains were lost during the preparation of the SEM.
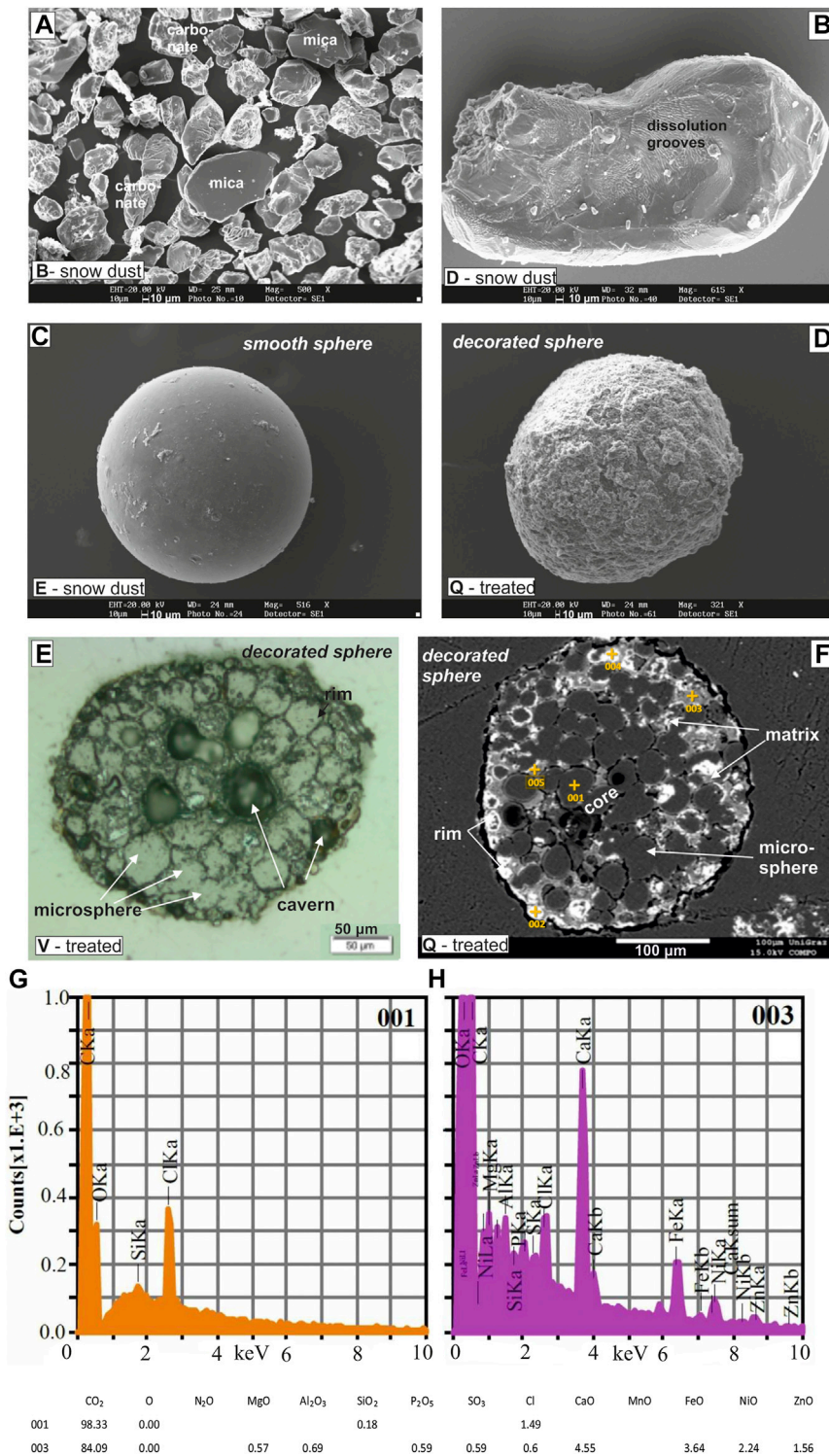
FIGURE 2 | (A) Overview of various mineral grains by scanning electron microscope. **(B)** Etched quartz grain and their surfaces. **(C)** Perfect sphere with a smooth surface interpreted as a micrometeorite. **(D)** Sphere with decorated, grainy surface interpreted as fly ash (see discussion). **(E,F)** Internal structure of the decorated spheres. **(A–D)** and **(F)** Scanning electron microscope, **(E)** Optical microscope. Representative EDS spectra of microspheres of samples 001 and 003 in Q2. **(G)** Microsphere is rich in carbonaceous material, oxygen, and some chlorine (location 001). **(H)** is from margin of the decorated microsphere and is rich in carbon, oxygen, calcium, and some other metals (location 003, see counts of elements below).

3) Decorated spheres: These were distinguished from smooth spheres (**Figure 2D**). In two samples (particularly in samples G and H, plant dust), there were a few bronze-colored spheres (both <100 μm and >100 μm), which could be interpreted as fly ash grains, as outlined in the SEM study. These spheres have a spherical shape similar to that of micrometeorite spheres (MMS), but the texture with a grained surface implies the presence of small mineral grains on the surface. The decorated spheres showed a gradual transition to drop-like shapes with a broken conic bulge and a fine-grained, rough crystallized surface. The largest grains ranged in size from 350 to 450 μm. Optical microscopy revealed that the surface layer appeared brownish to rusty, indicating the involvement of iron and/or manganese. These decorated spheres occurred in several samples collected from leaf surfaces, snow, and treated surfaces (**Table 1**). Most of these spheres were separated, embedded in epoxy, and cut through the center. Microphotographs of these central cuts revealed similar internal features of all decorated spheres, with small (10–35 μm) isometric microspheres embedded in a very fine-grained matrix, and common internal cavities (**Figures 2E–F**). These spheroidal grains spheres will be referred to as the small parts microspheres. Internally, the spheres are often not entirely filled with microspheres (**Figures 2E–F**); some are even empty inside but bear a rim, which is a zone of altered material. The microspheres were slightly deformed, implying that they were deformed in a soft state (**Figures 2E–F**). A fine-grained, partly cavernous matrix was found between the microspheres. In all cases, an alteration rim of reflective metal-rich material (FeO, MnO, and/or Fe-Mn-hydroxides) was observed along the margins of the spheres, implying some alteration after the formation and aggregation of microspheres into spheres. These rim zones are essential for the mechanical stability of the spheres.

To study the chemical composition of the sub-spheres and altered rims, many semi-quantitative chemical analyses were performed using the JEOL EDS system at the University of Graz, Austria. All measured points contained very rich carbon, which was then calculated as oxides, CO_2, and almost all other elements except Cl, and the sum was calculated as 100%. There are two types of microspheres (**Figure 2**): Type 001, consisting primarily of carbon (note that hydrogen cannot be measured using this method), were the most common. This type usually includes variable, low Cl and S content and P_2O_5. Type 001 microspheres gradually grade into Type 003 microspheres with high FeO (approximately 70%) and significant MnO content. The other components are NiO, MgO, CaO, and TiO_2. In some analyses, FeO was replaced by high MnO content. In general, the measured microsphere compositions at the rims of the sphere bear higher CaO and MnO contents. Decorated grains were observed in the snow dust and treatments.

The following types of mineral grains likely originate from the surrounding area (*in-situ* sources) (**Figure 2A**):

a) Quartz grains have smooth, structure-free surfaces and are generally angular (**Figure 2A**). A peculiar quartz aggregate showed a larger grain with a wing-like extension on one side, which is interpreted as a pressure fringe typical of low-grade metamorphic rocks. In a few cases, rounded quartz grains with pitted surfaces could be observed, and these few grains can be interpreted to result from long-distance aeolian transport.

b) Muscovite (maximum particle size: 250 μm × 500 μm) is recognized by its flakes with a perfectly smooth surface and internal cleavage (**Figure 2A**).

c) Amphibole is a prismatic mineral with a well-developed internal cleavage system and was found in sample H. EDX analysis indicated that Si, Mg, Ca, and O were the major constituents, whereas Al was not found.

d) Dolomite is discernible by the cleavage and cleavage planes on the surface. The grains were always angular, and no rounded surfaces were detected.

e) Calcite, with a particle size of approximately 850 μm × 650 μm, has a better cleavage system than dolomite and is often dissolved at the surface, displaying a slightly porous surface (**Figure 2A**).

f) Anorthite is an angular grain with spaced cleavage planes, and is slightly dissolved along the cleavage planes. EDX analysis revealed Ca, Al, Si, and O ($CaAl_2Si_2O_8$) as the main constituent elements, suggesting that plagioclase is close to the anorthite end-member.

g) Fe-oxide: Although slightly elongated, an apparent cubic, often sub-idiomorphic mineral with smooth surfaces, shows only Fe and O in the EDX analysis, implying the presence of magnetite (Fe_3O_4). Other Fe-rich ore minerals may represent hematite (Fe_2O_3) or iron hydroxide mixtures, including goethite. The particle sizes were 120–350 μm. The reddish-brown dust contamination on the snowpacks often considered "Saharan dust," is more likely iron-rich material from adjacent outcrops, supplemented by red-pigmented green algae that could be identified under the microscope.

h) Clay minerals are difficult to discern and were found in only a few samples: C, D, and E (snow dust); I, J, and K (plant dust); and O (treatment plot).

Representative images of dust particle shapes and their mineralogical composition analyzed by SEM-EDX or other imaging techniques are limited. Dong et al. (2014), for example, presented images of dust particles in China, showing different minerals (such as quartz, albite, kaolinite) and spherical fly ash particles dominated by silicon.

Dust Events and Dust Loads in the Vicinity of the Sonnblick Observatory

For the entire period (2013–2019), the Sonnblick Observatory recorded 21–29 days of dust events per year. In 2014, when most of the survey was conducted at Hochtor, dust events occurred over 24 days, 8 in spring and 16 in autumn and winter (Schauer, personal communication). The identification of long-distance transport dust at Sonnblick Observatory shows a significant increase in both the mass and relative concentrations of coarse particles (Schauer et al., 2016; Baumann-Stanzer et al., 2019). However, during the measurements at Sonnblick Observatory, the area was largely covered with snow, but not completely excluding the influence of local dust. Chemical analysis of a time series of snow samples collected near the Sonnblick

TABLE 2 | Main analytical data (arithmetic means and standard errors) of treatment and soil samples (2012, 2014, and 2020) at the Hochtor ($n = 5 –10$). Same of the data have already been published in (Peer et al., 2021).

	Treatment	pH	EC µS/cm	TOC %	TN %	Avail. P mg/kg	Avail. K mg/kg	Avail. Ca mg/kg	Avail. Mg mg/kg
2012	Bare soil	7.36 ± 0.06	88 ± 9.89	0.76 ± 0.31	0.06 ± 0.03	1.62 ± 1.03	6.96 ± 2.9	1696.7 ± 849.33	278 ± 179.96
2014	New crust	7.39 ± 0.03	124.36 ± 10.3	1.34 ± 0.51	0.15 ± 0.05	1.85 ± 0.42	10.69 ± 5.12	1763.5 ± 827.44	261.5 ± 91.99
2020	New crust	7.44 ± 0.05	94 ± 7.96	3.48 ± 1.48	0.2 ± 0.09	5.4 ± 1.81	24.6 ± 7.50	1897.2 ± 991.77	261.2 ± 22.89
	Undisturbed soil		µS/cm	%	%	mg/kg	mg/kg	mg/kg	mg/kg
2014	Topsoil	7.32 ± 0.03	169.28 ± 34.11	4.28 ± 5.22	0.18 ± 0.14	10.15 ± 8.21	28.88 ± 13.38	1950.4 ± 353.38	344.5 ± 12.47
2014	Subsoil	7.41 ± 0.04	87.9 ± 15.54	1.20 ± 144	0.08 ± 0.04	5.48 ± 6.74	8.15 ± 6.15	2049.3 ± 511.44	341.2 ± 85.86
2020	Topsoil	7.47± 0.03	96.5 ± 2.12	3.7 ± 0	0.2 ± 0.01	16 ± 0.01	42.5 ± 6.36	1574 ± 73.53	231.5 ± 9.18

	Treatment	Sand %	Coarse silt %	Medium+fine %	Silt %	Clay %	Texture
2012	Bare soil	56.98 ± 5.05	36.37 ± 11.16	4.99 ± 2.99	41.36	2.3 ± 1.13	sL
2014	New crust	58.69 ± 7.08	33.73 ± 7.86	5.28 ± 1.29	39.01	3.07 ± 0.89	sL
2020	New crust	75.26 ± 5.34	18.2 ± 5.63	3.34 ± 1.03	21.54	3.22 ± 0.58	lS
	Undisturbed soil	%	%	%	%	%	
2014	Topsoil	57.97 ± 5.95	37.01 ± 5.72	5.53 ± 4.65	34.04	2.56 ± 1.48	sL
2014	Subsoil	58.86 ± 7.08	27.90 ± 5.07	4.05 ± 5.36	31.81	3.52 ± 3.49	sL
2020	Topsoil	76 ± 12.3	19 ± 11.03	2.25 ± 0.91	21.25	2.85 ± 0.35	lS

2020	Fe mg/kg EDTA	Mn mg/kg EDTA	Cu mg/kg EDTA	Zn mg/kg EDTA	Ca^{2+} cmolc/kg	Mg^{2+} cmolc/kg	K^+ cmolc/kg	Al^{3+} cmolc/kg	Fe^{3+} cmolc/kg	Mn^{2+} cmolc/kg	CEC cmolc/kg
Treatment	228.8 ± 66.24	484.8 ± 448.26	1.5 ± 0.5	3.46 ± 1.35	9.48 ± 4.95	2.98 ± 1.47	<20	0.06	0.06 ± 0.01	<0.01	12.67 ± 6.41
Control	200.5 ± 16.26	305.5 ± 81.31	2 ± 0.42	9.15 ± 2.75	7.87 ± 0.36	2.49 ± 0.02	<20	0.06	0.045 ± 0.0	<0.01	10.85 ± 0.38

Observatory proves the regular impact of Saharan dust on glaciers (Greilinger et al., 2018). Soil sampling at Hochtor took place in July and September, by which time most of the snow patches has already disappeared. Therefore, in mineralogical analyses of the sieve fractions <100 µm and >100 µm, angular grains of predominantly local origin dominate the spectrum. Only a few typical round quartz grains with a porous surface were identified. These are most likely related to the North African deserts, although back-calculations could not be done due to the lack of data. We, therefore, concluded that distant grains are more or less completely diluted by local sources.

Soil Chemistry, Soil Types, and the Formation of Biological Soil Crusts

Compared with bare soil, the values of TOC, TN, available aP and aK, and EC increase slightly from 2012 to 2014 and continue to increase until 2020 (**Table 2**). Soil variables show different slope coefficients but were converted to annual growth rates, the average value for the first 2 years is 27.7%, and for the next 6 years, it is 20.5%. The annual growth rates of biocrust and aP are the highest from 2014 to 2020 at 32.8% and 32%, respectively. TOC increases by 26.5%, aK by 21.6%, and sand by 4.6%. However, the annual growth rate of nitrogen at only 5.5% is remarkable, because N-fixation is expected to increase with organic crust growth. (**Table 3**; **Figure 3**). The other parameters remain constant. The

TABLE 3 | Percentage increase in calculated crust and soil parameter values for each year between 2012–2014 and 2014–2020 (individual and average of all parameters).

	2012–2014 Period	2014–2020 Period	2012–2014 Per year	2014–2020 Per year
crust	37	197	18.5	32.8
TOC	76	159	38	26.5
TN	150	33	75	5.5
aP	14	192	7	32
aK	53	130	26.5	21.6
sand	3	28	1.5	4.6
mean value	55.5	123.6	27.75	20.5

soil texture varies from weak to strong silty sand, and the clay content is low. The cation exchange capacity (CEC) is quite low, slightly higher in treatments than in controls, with the highest percentages of Ca and Mg ions at 74.6% and 23.5%, respectively. The pH value is approximately 7.4. However, the EDTA values of iron and manganese indicate a high mobilization rate, which is higher in treatments than in controls (**Table 2**).

Despite the inhomogeneity of the parent material, airborne mineral particles (<100 µm and >100 µm) are confirmed by dust analysis of treatments (**Table 1**). The organic matter content and nutrient levels (N, aP, aK) are higher in undisturbed soils on

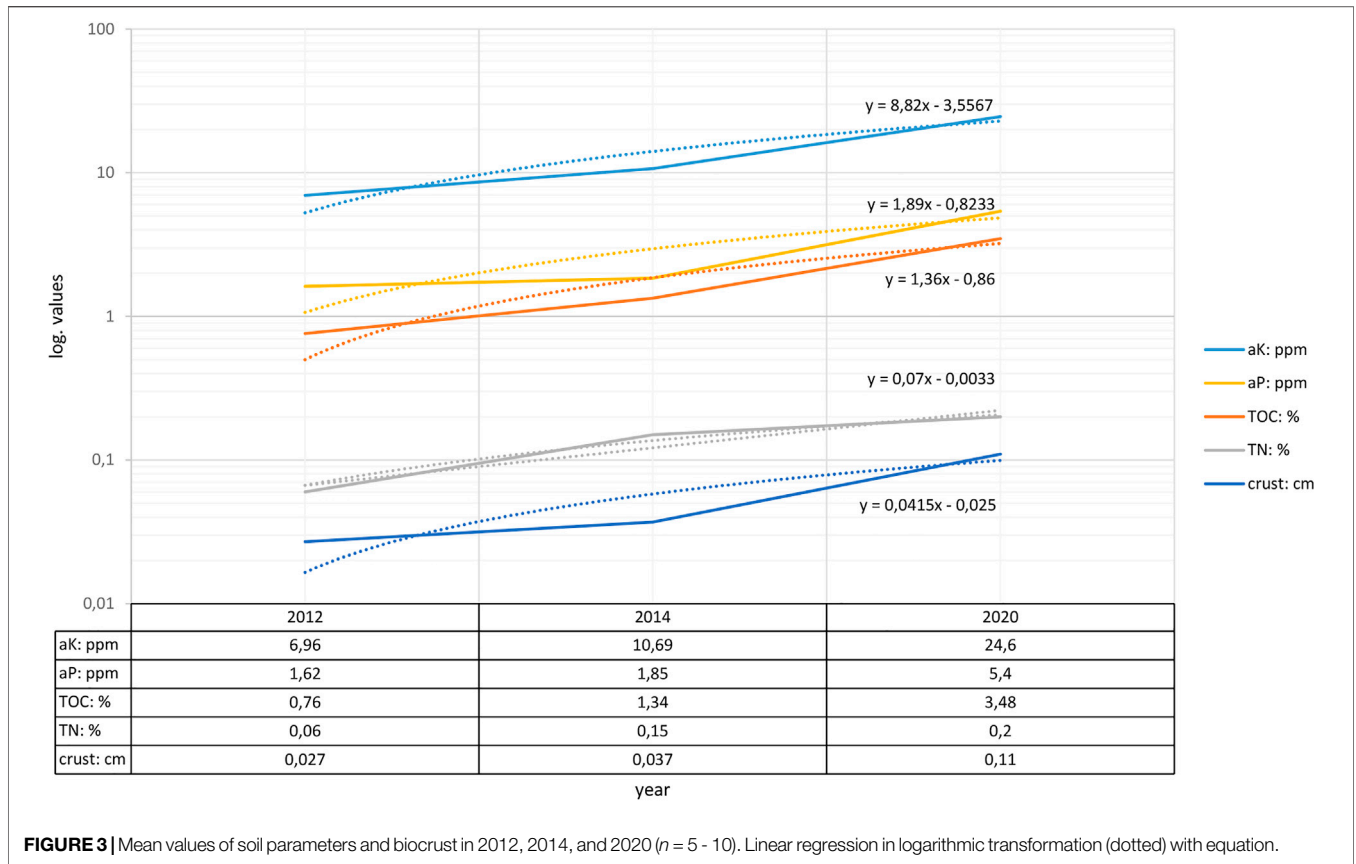|	2012	2014	2020
aK: ppm	6,96	10,69	24,6
aP: ppm	1,62	1,85	5,4
TOC: %	0,76	1,34	3,48
TN: %	0,06	0,15	0,2
crust: cm	0,027	0,037	0,11

FIGURE 3 | Mean values of soil parameters and biocrust in 2012, 2014, and 2020 (n = 5 - 10). Linear regression in logarithmic transformation (dotted) with equation.
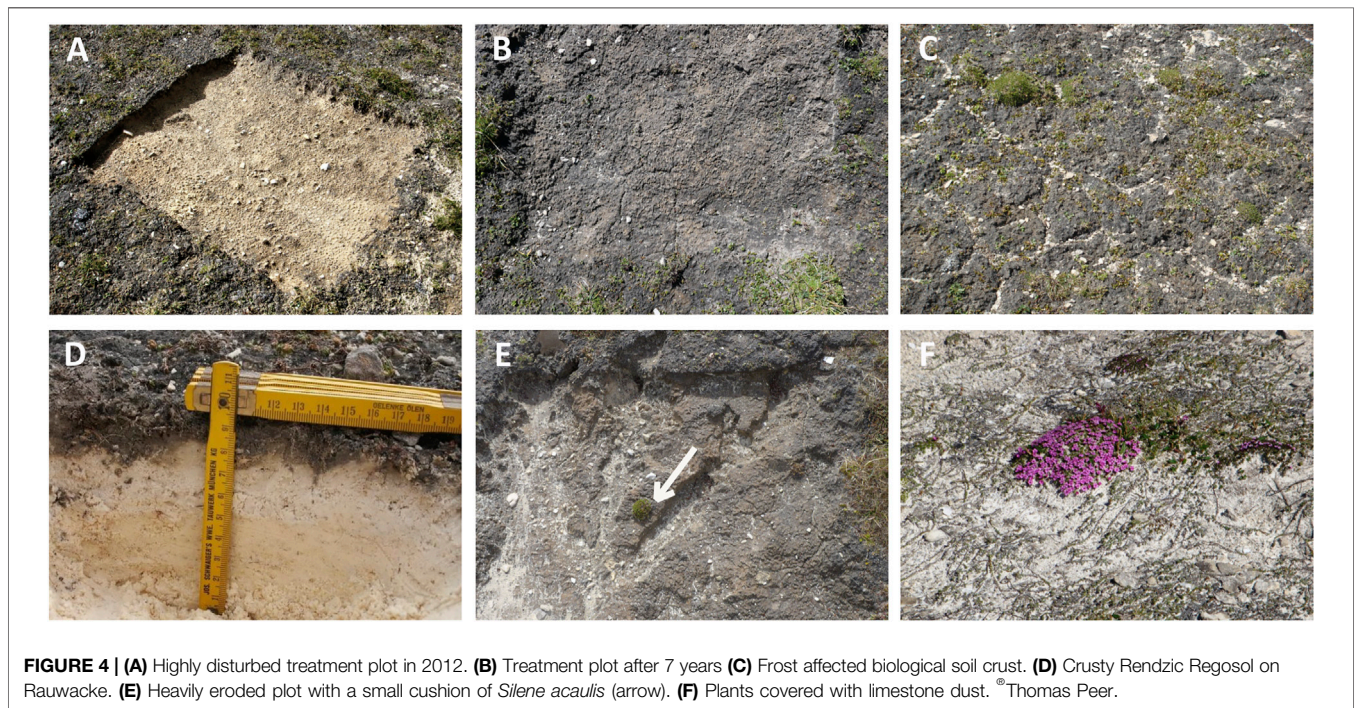

FIGURE 4 | (A) Highly disturbed treatment plot in 2012. **(B)** Treatment plot after 7 years **(C)** Frost affected biological soil crust. **(D)** Crusty Rendzic Regosol on Rauwacke. **(E)** Heavily eroded plot with a small cushion of *Silene acaulis* (arrow). **(F)** Plants covered with limestone dust. [®]Thomas Peer.

TABLE 4 | Plant species, mean number of individuals (2016–2020), slope coefficient, Pearson correlation coefficient (PCC), and coefficient of determination (R^2).

	2016	2017	2018	2019	2020	Slope	PCC	R^2
Braya alpina	5.4	6.6	9.1	12.1	9	1.11	0.739	0.547
Salix herbacea	5.8	4	6.87	10.14	10.71	1.59	0.881	0.776
Saxifraga oppositifolia	2.9	2	3	3.8	3.6	0.32	0.717	0.514
Persicaria vivipara	3.5	2	4.75	6.14	5.42	0.79	0.769	0.592
Ranunculus alpestris	3.8	2.6	3.55	3.52	2.28	−0.23	−0.59	0.348
Minuartia gerardii	0.6	4.6	4.55	8.12	4.5	1.13	0.676	0.452
Silene acaulis	2.9	3.9	2.7	2.2	2.2	−0.31	−0.7	0.493
Euphrasia minima	0.2	0.8	0.7	0.5	1.5	0.23	0.733	0.567
Primula minima	1	0.8	0.6	1	0.5	−0.08	−0.56	0.307
Sesleria ovata	0.4	0.6	0.8	1.5	0.7	0.15	0.556	0.31

rauwacke than in the treatments, and in the topsoil than in the subsoil, with a few exceptions. Since 2012, a thin, discontinuous layer of cyanobacteria (BSCs light color, early successional type; Belnap and Eldridge, 2003) has formed, transitioning to BSC dark (an advanced successional type, which contains a higher density of microbes) in 2020 (**Figures 4A,B**). During this period, the thickness of the crust layer increases from 0.027 ± 0.013 cm to 0.11 ± 0.028 cm.

For the first 8 years, soil formation and stratification could not be determined as there are no soil residues in the plots. However, in undisturbed sites, the soil corresponds to a crusty "Rendzic Regosol" (**Figure 4D**), which we have described in previous studies (Peer et al., 2010; Zheng et al., 2014). The soil is 20–30 cm deep, the humus layer is 5–15 cm deep, and the crust covers 0.2–1 cm. The soil has mainly developed from indigenous material and has only been slightly modified by wind admixtures. These include the transport of fine sand and the significant increase in some nutrients (aP and aK) and TOC. Silt was the only parameter that decreased during the 8-years observation period. In contrast, allochthonous silt significantly affects topsoil in the Northern Limestone Alps (Küfmann, 2008a; Grashey-Jansen et al., 2014; Mix and Küfmann, 2015). Alpine Cambisols and alpine Luvisols occur in alpine meadows on compact dolomitic and limestone marbles. The clay content increases with increasing depth, indicating residues of local bedrock and/or allochthonous periglacial sediments during the Holocene (Gračanin, 1972; Biermayer and Rehfuess, 1985; Küfmann, 2008a). According to Munsell soil color charts, the color of the solum is sometimes slightly reddish (between 2.5YR and 5YR). Such chromic Cambisols have also been identified by Solar (1964), Biermayer and Rehfuess (1985), and Küfmann (2008b) in alpine karst areas.

Plant Composition and Plant Growth.

In treatments, the estimated cover rate of vascular plants is generally less than 1%. Most individuals are between 0.1 and 2 cm in height, and most of them are vegetative. Although the dominance ratio is different, annual species composition and number (an average of 9–13 species per plot) are similar. However, from 2016 to 2020, the number of individuals increases slightly with some exceptions, and the calculated regression slope coefficients range from −0.31 to 1.59. Although the correlation between individuals and years is
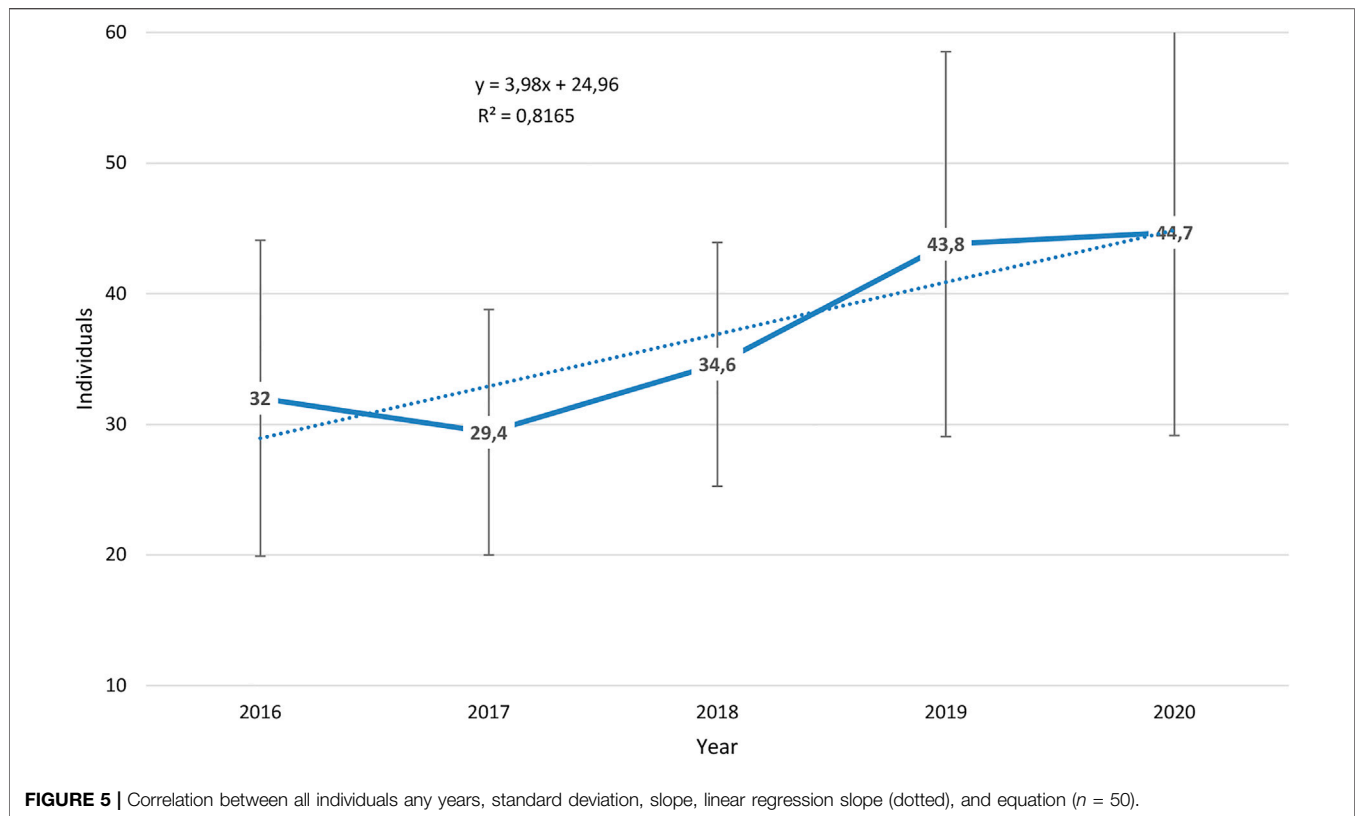
relatively strong ($r > 0.5$), R^2 values between 0.31 and 0.77 appear to be widespread near the regression line (**Table 4**). For all individuals and plots, the slope coefficient is 3.98, indicating a better fit (**Figure 5**).

Common species are *Braya alpina* (endemic in the Eastern Alps), *Minuartia gerardii*, *Saxifraga oppositifolia*, *Salix herbacea*, *Persicaria vivipara*, *Ranunculus alpestris*, *Sesleria ovata*, and *Silene acaulis*. Most species grow separately, partly in groups, and often follow cracks and crevices where detritus and fine material are washed into them, thereby creating a better milieu for germination (**Figure 4C**). Others move in from the edges, such as *S. oppositifolia* through long runners or creeping plants such as *S. herbacea* and *Dryas octopetala*. Calcareous species are the most abundant (46.7%), followed by intermediate plants (33.3%), and acidophilic species (20%) such as *P. minima*, *Euphrasia minima*, and *S. herbacea*. The white lime dust cover on the plants is shown in **Figure 4F**. Lichens and bryophytes were not detected in the first years. However, 19 to 22 different plant species were found in undisturbed plots, with a coverage rate of approximately 25%, lichens 20%–30%, and bryophytes less than 10%. BSCs usually account for 50% or more of the area and are mainly composed of cyanobacteria, including species of *Microcoleus*, *Croococcus*, *Gloeocapsa*, and *Nostoc*. In addition, cyanolichens (with cyanobacteria as the photosynthesizing component), such as *Collema* spp. and *Peltigera* spp., have the potential for nitrogen fixation (Zheng et al., 2014; Williams et al., 2016).

DISCUSSION

Rare Minerals, Volcanic Phenocrysts, Tektites, Micrometeorites, and Fly Ashes

Aeolian dust particles carried by the wind from *in-situ* weathering rocks of the Hohe Tauern, volcanic eruptions, impact craters, North African deserts, or even from space, are important constituents of the high alpine area of the Hochtor. Aeolian dust is deposited on soils, BSCs, treatment plots, vegetation, and snowpacks. Assessment of the mineralogical components revealed a mix of dominance of locally and regionally derived grains, and subordinate potentially far-traveled exotic grains such as volcanic quartz phenocrysts, spheres from anthropogenic sources (see below), microtektites, and micrometeorites, the

FIGURE 5 | Correlation between all individuals any years, standard deviation, slope, linear regression slope (dotted), and equation ($n = 50$).

latter also being considered "cosmic dust" of extra-terrestrial origin. In summary, in terms of relative proportion, local mineral grains dominate the composition of the dust, including typical minerals of the Hohe Tauern, such as calcite and dolomite from marble, calcareous mica schists, subordinate greenschists, amphibolites, and serpentinites (Höck, 1980; Schmid et al., 2013). Small amounts of opaque ore minerals are commonly found in metamorphic, magmatic, and sedimentary rocks, which represent a metamorphic primary magmatic assemblage modified by supergene alteration during the Alpine orogeny (Ramdohr, 1969; Ashley, 1975).

Volcanic phenocrysts may be related to volcanic shards, but there are no clear fragments with characteristic concave surfaces, sharp edges, and irregular tetrahedral shapes, and their occurrence is not completely excluded. The development of the peculiarly etched quartz surface is still entirely unknown and appears to be chemically leached, possibly because of the textures caused by chemical abrasion during grain transport in aeolian environments (Krinsely et al., 1976; Newsome and Ladd, 1999; Woronko et al., 2015; Kalińska et al., 2017).

The following discussion of decorated spheres is centered around two points: 1) the fabrics of decorated spheres, which are composed of microspheres, and 2) the chemical composition of the microspheres. The fabric of the decorated spheres indicates that they represent the agglomeration of small microspheres of mostly carbon-dominated materials. The microspheres resemble carbon-dominated fly ashes, which are known to originate from burning coal or formed during cement production (Brindle and

McCarthy, 2006; Kutchko and Kim, 2006; Alergiczny, 2019). Additionally, fly ash is generally composed of amorphous glass. Although there are some differences (such as fly ash microspheres being cavernous), no agglomeration was observed in our samples. However, most studies on fly ash have been performed on pristine material at the source, but not after long aeolian transport. The composition of microspheres of decorated spheres is dominated by carbon, which could be organic carbon or solid hydrocarbons, pure carbon, or simply graphitic carbon, as defined by metamorphic carbon matter (Beyssac and Rumble, 2014). A well-known environmental problem is the presence of black carbon in the atmosphere due to burning of hydrocarbons and coal (Ramanathan and Carmichael, 2008). Small amounts of Cl and S could also result from the burning process. Zierold and Odoh (2020) demonstrated that a large range of metals, including Fe, Mn, Ti, Ni, and Zn, contribute to fly ash, including those observed in our samples. Based on textural observations and the chemical composition of microspheres, we suggest that the decorated spheres are aggregates of fly ashes of anthropogenic origin, potentially from a metal-producing factory and a power plant.

Significantly unique, perfect spheres with a completely smooth surface could have two different sources: the spheres with a smooth and polished surface, representing micrometeorites that come directly from space (cosmic dust); and the glassy spheres such as the tektites, which are now recognized to have been created by the melting and rapid cooling process of terrestrial rock that was vaporized by high-

TABLE 5 | Eigenvalue, variability, and cumulative variability explained by factor analysis (6 factors) using correlation matrix on the measured attributes. The eigenvalue of F1 is 4.469, whereas the eigenvalues of the other factors are all less than 1. The cumulative first three factors account for almost 67% of the total variation. This shows that these three factors define the most variability and can be used as replacements for other factors.

	F1	F2	F3	F4	F5	F6
Eigenvalue	4.469	0.852	0.711	0.093	0.048	0.015
Variability%	49.659	9.468	7.901	1.032	0.539	0.167
Cumulative variability%	49.659	59.128	67.028	68.061	68.600	68.767

TABLE 6 | Factor loadings and communality of nine soil variables in relation to the three factors.

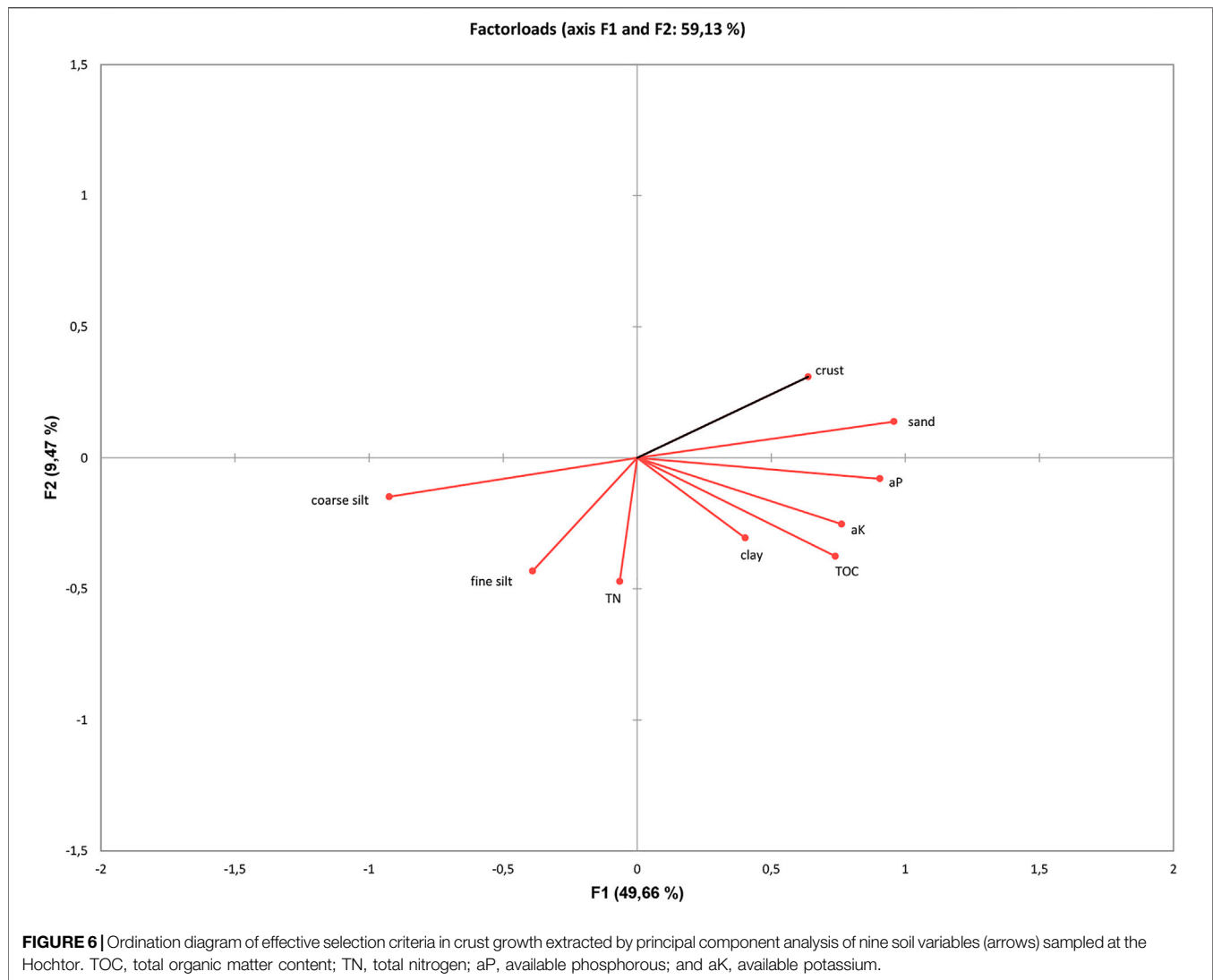| Variables	F1	F2	F3	Communality
Crust	0.523	0.432	0.064	0.464
TOC	**0.666**	−0.350	−0.181	0.599
TN	0.404	−0.531	0.023	0.445
aP	**0.911**	−0.151	0.384	1.000
aK	**0.656**	−0.486	0.215	0.713
Sand	**0.936**	0.256	0.095	0.951
Coarse silt	−0.912	−0.337	0.236	1.000
Fine silt	−0.281	−0.537	−0.193	0.404
Clay	0.482	−0.054	−0.696	0.721

Bold: Soil variables with the highest positive values within F1.

energy impacts of large meteorites on the Earth's surface. The clouds of molten silicate droplets quickly cool to a glassy form before falling back to Earth (Eiby, 1959; Faul, 1966; Bouška, 1968; Glass, 1990; Koeberl, 1990; Koeberl, 1994; French and Koeberl, 2010; King, 2020). The scarcity of known strewn fields regarding the number of identified impact craters indicates the special and rare circumstances under which tektites are formed by meteorite impact (King, 2020). According to Ernstson et al. (2014) and Rappenglück et al. (2017), the microtektite-like glasses probably originate from the Northern Calcareous Alps, from the Holocene Chiemgau meteorite crater stream field. Several experts (O'Keefe, 1966; Fehr et al., 2005; Schüssler et al., 2005; Prasad et al., 2013) do not approve this hypothesis as they expect other localities and crater strewn fields to be much older (millions of years before present). Moreover, our semiquantitative EDX analysis does not include determination of the source impact crater due to the different geological conditions and oxide ratios of the respective impact craters (Lowman, 1962; Bouška, 1968; Glass, 1990; Köberl, 1990; Köberl, 1994). However, MMs are extraterrestrial particles (cosmic dust) that survive atmospheric entry and reach the Earth's surface (Genge et al., 2008). MMs are in the size range of 25–400 µm and are found on plant surfaces, although their grain size is relatively large. This observation could potentially be used to search for micrometeorites at higher elevations. Many types of MMs change in appearance and chemism when heated upon entry into the atmosphere (Glass, 1990; Folco and Cordier, 2015). In addition, the unusual ratios of many other metals (such as platinum-group elements) in relation to their environment indicate their extraterrestrial origin (Taylor et al., 2016). It is assumed that an explosion caused by the airburst of an asteroid triggered MMs. Their annual input is estimated to be 37,000–78,000 tons, mainly recovered from deep-sea sediments, Antarctic ice, deserts, and loose sediments in polar areas (Love and Brownlee, 1983; Brownlee, 1985; Folco and Cordier, 2015). Cosmic spherules with melted quartz and pyroxene grains, carbon spherules, and glass-like carbon have also been found in the Late Pleistocene paleosols of the Western Alps (Mahaney et al., 2017). In the case of the Tunguska event, which occurred in the Eastern Siberian taiga in 1908, cosmic material was distributed over a wide area, triggered by an enormous explosion caused by the impact of a small asteroid (comet or meteorite) on the Earth's atmosphere (Badyukov et al., 2011). However, there are still discrepancies regarding the origin of the cosmic material that has accumulated in the peaty soils of Central Siberia. According to some experts (Ganapathy, 1983; Zbik, 1984), iron-rich spherules are only partially linked to the Tunguska event and are more likely to originate from the steady cosmic incursion.

TABLE 7 | Spearman correlation matrix ($p \leq 0.05$) of crust and selected soil parameters.

Variables	Crust	TOC	TN	aP	aK	Sand	Coarse silt	Fine silt	Clay
Crust	1	0.136	−0.073	0.493	0.147	0.611	−0.629	−0.309	0.200
TOC	0.136	1	0.418	0.595	0.568	0.546	−0.557	0.054	0.456
TN	−0.073	0.418	1	0.449	0.529	0.296	−0.200	0.179	0.206
aP	0.493	0.595	0.449	1	0.767	0.829	−0,677	−0.232	0.186
aK	0.147	0.568	0.529	0.767	1	0.482	−0.400	0.025	0.195
Sand	0.611	0.546	0.296	0.829	0.482	1	−0.914	−0.461	0.363
Coarse silt	−0.629	−0.557	−0.200	−0.677	−0.400	−0.914	1	0.436	−0.599
Fine silt	−0.309	0.054	0.179	−0.232	0.025	−0.461	0.436	1	0.045
Clay	0.200	0.456	0.206	0.186	0.195	0.363	−0.599	0.045	1

FIGURE 6 | Ordination diagram of effective selection criteria in crust growth extracted by principal component analysis of nine soil variables (arrows) sampled at the Hochtor. TOC, total organic matter content; TN, total nitrogen; aP, available phosphorous; and aK, available potassium.

Pedogenesis and Biological Soil Crusts in Response to Dust. What Factors Contribute to the Surprisingly Fast Growth of Biological Soil Crusts?

Nutrient limitation is considered a key factor affecting microbial community assembly and microbial growth and is also critical to the growth of biological crusts (Yoshitake et al., 2007; Williams et al., 2016; Williams et al., 2017; Vinšová et al., 2018; Banerjee, 2021). However, research shows that mineral dust can make up for nutrient deficiencies (e.g., Mladenov et al., 2012; Lin and Feng, 2015; Greilinger et al., 2018; Di Mauro et al., 2019). Ciccazzo et al. (2005) and Rime et al. (2016) studied the early succession of high mountains and indicated that atmospheric deposition is an important source of dissolved organic carbon, nitrate, and ammonium. According to Schmidt et al. (2008), and other authors, cyanobacterial diversity increases significantly in the first four consecutive years following glacier retreat, with both aeolian deposition and cyanobacterial activity contributing to the accumulation of carbon and nitrogen. Based on these findings and our SEM-EDX results, we hypothesized that nutrient loads associated with airborne particles, clay minerals, and humus contribute to the rapid growth of BSC only 2 years after complete soil removal. Over the next 6 years, the early light-colored biocrust turned into a well-developed dark-colored biocrust, along with an increase of nutrients and organic matter content. As proven in **Table 2**, aP, aK, TN, and organic matter content increased significantly from 2014 to 2020, which can also be attributed to the subsequent factors: 1) decomposition of organic substances; 2) mineral weathering processes; and 3) input of dust particles, particularly in the fraction of fine sand that provides additional nutrients. The year-round high humidity and fine-grained substrate are thought to be further reasons for the rapid crust development at Hochtor. Measurements of photosynthesis in the crust prove that despite the long snow cover, microorganisms are active year-round, forming a moderately tick-shaped crust over time (Büdel et al., 2014; Rozenstein et al., 2014; Weber et al., 2016; Williams

et al., 2017). BSCs subsequently improve the physical and chemical properties of the underlying soil by accumulating organic matter, fixing nitrogen, increasing aggregate stability, and water retention, thereby protecting the soil from wind and water erosion, thereby affecting the hydrological cycle in these ecosystems (Evans and Johansen, 1999; Belnap et al., 2001; Belnap, 2003; Belnap and Lange, 2003; Belnap, 2006; Breen and Lévesque, 2008; Yang et al., 2014; Maestre et al., 2016; Canton et al., 2020).

The factor analysis model generated for the first two dimensions illustrates the structure of the dependence and the interrelationships between the selected soil parameters and the biocrust (a total of nine variables). As shown in the graph in **Figure 6**, the first-factor loading explains 49.6% of the total variance, and the second-factor loading explains 9.4% of the total variance. The percentage of total variance explained by the two components is 59.13%. F1 involves most of the parameters, such as sand, aP, aK, and TOC, and is positively correlated with the biocrust, whereas coarse silt and fine silt are negatively correlated. F2 is affected by TN and has a low negative correlation with the biocrust, which we cannot yet interpret. Finally, in F3, only clay has the highest weight (**Tables 5, 6**). In the Spearman correlation matrix, sand and aP have the highest correlation with biocrust, although their values are only 0.611 and 0.493, respectively (**Table 7**). However, it can be inferred from the statistical analyses that sand, aP, aK, and TOC may have an impact on the biocrust, which can also be seen from the communality values (**Table 6**). As shown in **Table 3**, the annual rates of increase of aP, aK, and TOC are the highest between 2014 and 2020. The statistical proximity of available phosphorus to the biocrust can be considered essential for the microbial growth of the biocrust (Sharma et al., 2013).

The infiltration of fine sand along the surface frost cracks (**Figure 4C**), plant detritus, and organic matter content improve the physical, chemical, and biological properties of the soil, turning the raw gravel soil into a crusty Rendzic Regosol with a notable A-horizon (Huber et al., 2007; Zheng et al., 2014). A high proportion of fine sand (less silt) and mica minerals on the surface and in the subsurface soil may imply the contribution of aeolian dust (Grashey-Jansen et al., 2014). However, the texture difference in the well-weathered rauwacke profile is still unclear, and the texture of the solum is quite similar to that of the bedrock. On the other hand, significant differences in texture were observed in other alpine areas, indicating aeolian input. However, the assessment of the sources of mineral dust is interpreted differently in the international literature. For example, Rapp (1984), Küfmann (2003), Küfmann, 2008a, Küfmann, 2008b), Jahn (2010), and Varga et al. (2016) emphasized the co-influence of Saharan dust on pedogenesis, while other scientists, such as Yaalon and Ganor (1973), Sticher et al. (1975), Biermayer and Rehfuess (1985), Johnston (2001), and Lin and Feng (2015), assumed local sources from various nearby bedrock areas. In addition to recent dust accumulation, loess deposits from the late glacial period can also serve as soil-forming admixtures (Küfmann, 2003; Muhs and Benedict, 2006; Gild et al., 2017). Based on our mineralogical (SEM-EDX) and pedological data (soil

chemistry, grain size), it can be concluded that aeolian dust participates in the accelerated growth of BSCs and soil formation.

How Does Dust Affect Plant Growth and Plant Composition, and What Does Dust Have to Do With the Occurrence of Silicate Plants in Limestone Environments?

As assumed during initial soil formation, dust input also affects plant growth, shaping the soil environment and enhancing water and nutrient properties, thereby promoting vascular plant succession rates (Belnap et al., 2003). Colonization of the disturbed sites at Hochtor occurs partly with the germination of seeds, although most of them do not survive the harsh weather conditions in winter (as shown by the comparative counts in summer and after snowmelt). Moreover, fragments of plants carried by wind or water and runners of plants moving from the edges may have contributed to further colonization. As the treatments are permanently exposed to severe erosion (**Figure 4E**), the newly emerged plants are washed away or grazed by sheep and goats (as shown by the footprints). Only a few plants survive. This could explain the low increase in individuals from 2016 to 2020, despite adequate nutrition levels. Frequent disturbances, such as erosion, relocation of ground material, and frost movement, may initially inhibit lichen growth rates. This is thought to be the main reason why lichens have not developed for 7 years. On the other hand, lichens can also trap dust particles, and some epilithic species can incorporate dust into thalli and use it for metabolic processes, similar to BSCs (Jung et al., 2020). Both organisms are adapted to stressful habitats; however, comparative data are largely missing. At Hochtor, BSCs dominate many sites, together with lichens and vascular plants. In other places, lichens occupy more space, and vascular plants are displaced to the edges. However, vascular plants can also dominate, especially cushion plants, grasses, and plants that form ground mats where dust minerals accumulate (**Table 1**). This continuous change in the appearance of organisms can be regarded as a syndynamical process that has not yet been fully understood. Mineral dust may play a key role in this process as nutrients adjust to the different needs of plants and lichens. Species competition, allelopathy, resistance, and resilience are other factors that play a role in areas with large and small site variations (Körner, 1995).

The presence of acidophilic plants in a limestone environment is another characteristic of this area. We hypothesize that the iron and phosphorus deficiencies in limestone soil can be compensated for by airborne silicate minerals and fly ash, which are captured from alpine vegetation and dissolved over time. The availability of iron in the EDTA extract and the dissolved iron and phosphorus in snow water from dusty snow patches may be important sources. The comparative analysis of cell saps of two "acidophilic" plants, *P. minima* and *C. uniflorum*, reveals higher concentrations of Fe and Al in acidic soils, although the cell sap concentration in calcareous soils is nevertheless

sufficient for plant growth (Reitbauer, 2010). The high Ca and Mg concentrations in calcareous soils can be controlled by carboxylic acids (Kinzel, 1983). Therefore, the two acidophilic plants are classified as calcitolerant and slightly siderophilic ("metal-loving"), but not strongly acidophilic. Several studies have reported that airborne bacteria, fungal spores, pollen grains, and other bioparticles, which are associated with atmospheric dust, survive even at stratospheric altitudes and become active again in their new habitats (Kellogg and Griffin, 2006; Meola et al., 2015; Aguilera et al., 2018; Greilinger et al., 2018). In addition, fragments and propagules of BSCs are likely to be present in the atmosphere and transported long distances by dust storms, potentially acting as a source for the "passive restoration" of soil crusts (Rossi et al., 2017; Warren et al., 2019).

On a global scale, there is increasing awareness of the importance of dust in terrestrial and aquatic ecosystems. It provides nutrients, such as phosphorus and nitrogen, as well as trace metals, such as iron, manganese, titanium, and aluminum (Goudie and Middleton, 2006). Mineral dust affects the growth of plants in rainforests, thereby balancing poor rainforest soils (Okin et al., 2004; Rizzolo et al., 2016). Mineral dust fertilizes marine phytoplankton, thereby increasing marine primary productivity (Franchy et al., 2013), and, at least, mineral dust alters the competitive balance among community species due to its chemistry and pH value (Farmer, 1993). In alpine environments, local winds disperse calcareous and siliceous mineral dust to different places, forming microhabitats, thereby increasing species richness through the presence of calcicole and calcifuge plants (Wohlgemuth and Gigon, 2003). This phenomenon is also observed at Hochtor and will be investigated in future studies. In the future, another problem will arise in alpine regions: due to global warming and rapid glacier retreat, the unvegetated glacial foreland will become larger, promoting more "alpine loess," and 2) due to increased drought (especially in the Mediterranean) more barren land and fires will be generated, which will change the composition of dust, leading to the chemical, optical and microphysical properties (Schauer et al., 2016).

CONCLUSION

Dust samples collected from snow patches, plants, and treatments include a variety of minerals, mainly from local and regional bedrock outcrops. Potential exotic grains are volcanic quartz phenocrysts and spherules, both tektites and micrometeorites (cosmic dust), as well as fly ash aggregates. Currently, dust input has a relatively limited effect on soil formation in Hochtor, but it contributes to a better supply of nutrients, with silicate minerals promoting acidophilic plants in limestone environments. Dust-derived nutrients also promote microbial growth and the rapid development of BSCs. It was found that fine sand and available

phosphorous are the main drivers of crust growth. The soil type has evolved from surface-consolidated gravel soil to Rendzic Regosol with a dark solid biological crust on the surface. BSCs subsequently improve the physical and chemical properties of the underlying soil by accumulating organic matter, fixing nitrogen, increasing aggregate stability, and water retention, thereby protecting the soil from wind and water erosion. Aeolian dust has been found to change alpine ecosystems by expanding habitats for plants and increasing biodiversity. However, with strong winds mixed near the main ridge, it was difficult to pinpoint the source of the dust. Therefore, the proportion of Saharan dust must be questioned.

The alpine area of Hochtor is a very fragile ecosystem, not only threatened by currently recognized climate change, but also by mechanical forces, such as cattle treads and trampling by hikers. Once damaged, BSCs may take many years to grow back. During this time severe erosion can cause lasting damage to the alpine landscape. Therefore, strict management activities are required to protect the area and prevent soil erosion and landslides, which threaten tourism and valuable pastures.

DATA AVAILABILITY STATEMENT

The raw data supporting the conclusion of this article will be made available by the authors, without undue reservation.

AUTHOR CONTRIBUTIONS

TP conceptualized the study, TP, FN, CH, and AK-G edited the manuscript and searched the literature. TP, L-JZ, FN, GF, CH, and AK-G participated in the analysis of the data. Fieldwork was performed by TP, L-JZ, FN, and GF. Sample analyses were performed by TP, L-JZ, FN, GF, and CH. The article was drafted by TP with contributions from all authors.

FUNDING

ACKNOWLEDGMENTS

REFERENCES

Aguilera, Á., de Diego-Castilla, G., Osuna, S., Bardera, R., Sor Mendi, S., Blanco, Y., et al. (2018). "Microbial Ecology in the Atmosphere: The Last Extreme Environment," in *Extremophilic Microbes and Metabolites Diversity Bioprospecting and Biotechnological Applications*. Editors A. Najjari, A. Cherif, H. Sghaier, and H. I. Ouzari (London, United Kingdom: Intech Open Online Open Access Books). doi:10.5772/intechopen.81650

Alergiczny, Z. (2019). Fly Ash and Slag. *Cem. Concr. Res.* 124, 105826. doi:10.1016/j.cemconres.2019.105826

Angelisi, M. D., and Gaudichet, A. (1991). Saharan Dust Deposition over Mont Blanc (French Alps) during the Last 30 Years. *Tellus B* 43, 61–75. doi:10.1034/j.1600-0889.1991.00005.x

Ansmann, A., Bösenberg, J., Chaikovsky, A., Comerón, A., Eckhardt, S., Eixmann, R., et al. (2003). Long-range Transport of Saharan Dust to Northern Europe: The 11-16 October 2001 Outbreak Observed with EARLINET. *J. Geophys. Res.* 108 (D24), a–n. doi:10.1029/2003JD003757

Ashley, P. M. (1975). Opaque Mineral Assemblage Formed during Serpentinization in the Coolac Ultramafic Belt, New South Wales. *J. Geol. Soc. Aust.* 22 (1), 91–102. doi:10.1080/00167617408728877

Auer, I., Böhm, R., Leymüller, M., and Schöner, W. (2002). *Das Klima des Sonnblicks – Klimaatlas und Klimatopographie der GAW Station Sonnblick einschließlich der umgebenden Gebirgsregionen.* Österr. Beitr. Meteorologie und Geophysik *28*. Wien: Zentralanstalt für Meteorologie und Geodynamik , 408.

Badyukov, D. D., Ivanov, A. V., Raitala, J., and Khisina, N. R. (2011). Spherules from the Tunguska Event Site: Could They Originate from the Tunguska Cosmic Body? *Geochem. Int.* 49 (7), 641–653. doi:10.1134/S0016702911070032

Banerjee, S. (2021). Microbial Growth and Nutrition. *J. Basic Microbiol. Biol. Notes*.

Baumann-Stanzer, K., Greilinger, M., Kasper-Giebl, A., Flandorfer, C., Hieden, A., Lotteraner, C., et al. (2019). Evaluation of WRF-Chem Model Forecasts of a Prolonged Saharan Dust Episode over the Eastern Alps. *Aerosol Air Qual. Res.* 19:6, 1226–1240. doi:10.4209/aaqr.2018.03.0116

Belnap, J., and Eldridge, D. J. (2003). "Disturbance and Recovery of Biological Soil Crusts", in *Biological Soil Crusts: Structure, Function, and Management*, eds. J. Belnap and O. L. Lange, 150. *Ecol. Studies* Springer, Berlin, 364–383.

Belnap, J., Kaltenecker, J. H., Rosentreter, R., Williams, J., Leonard, S., and Eldridge, D. J. (2001). *Biological Soil Crusts: Ecology and Management: TR–1730-2.* Denver, CO: US Department of the Interior.

Belnap, J., and Lange, O. L. (Editors) (2003). "Biological Soil Crusts: Structure, Function, and Management,". *Ecol. Stud.* (Berlin: Springer), 150, 503.

Belnap, J., Prasse, R., and Harper, K. T. (2003). "Influence of Biological Soil Crusts on Soil Environments and Vascular Plants", in *Biological Soil Crusts: Structure, Function, and Management*, eds. J. Belnap and O. L. Lange, *Ecol. Studies* 503, Springer, Berlin, 281–300.

Belnap, J. (2006). The Potential Roles of Biological Soil Crusts in Dryland Hydrologic Cycles. *Hydrol. Process.* 20, 3159–3178. doi:10.1002/hyp.6325

Belnap, J. (2003). The World at Your Feet: Desert Biological Soil Crusts. *Front. Ecol.* 1 (5), 181–189. doi:10.1890/1540-9295(2003)001[0181:twayfd]2.0.co;2

Beyssac, O., and Rumble, D. (2014). Graphitic Carbon: a Ubiquitous, Diverse, and Useful Geomaterial. *Elements* 10, 415–420. doi:10.2113/gselements.10.6.415

Biermayer, G., and Rehfuess, K. E. (1985). Holozäne Terrae fuscae aus Carbonatgesteinen in den Nördlichen Kalkalpen. *Z. Pflanzenernaehr. Bodenk.* 148 (4), 405–416. doi:10.1002/jpln.19851480405

Bouška, V. (1968). On the Original Rock Source of Tektites. *Lithos* 1, 102–112.

Breen, K., and Lévesque, E. (2008). The Influence of Biological Soil Crusts on Soil Characteristics along a High Arctic Glacier Foreland, Nunavut, Canada. *Arct. Antarct. Alp. Res.* 40, 287–297. doi:10.1657/1523-0430(06-098)[breen]2.0.co;2

Brindle, J. H., and McCarthy, M. J. (2006). Chemical Constraints on Fly Ash Glass Compositions. *Energy fuels.* 20, 2580–2585. doi:10.1021/ef0603028

Brownlee, D. E. (1985). Cosmic Dust: Collection and Research. *Annu. Rev. Earth Planet. Sci.* 13 (1), 147–173. doi:10.1146/annurev.ea.13.050185.001051

Büdel, B., Colesie, C., Green, T. G. A., Grube, M., Lázaro Suau, R., Loewen-Schneider, K., et al. (2014). Improved Appreciation of the Functioning and Importance of Biological Soil Crusts in Europe: the Soil Crust International Project (SCIN). *Biodivers. Conserv.* 23, 1639–1658. doi:10.1007/s10531-014-0645-2

Burger, R., and Franz, H. (1969). Die Bodenbildung in der Pasterzenlandschaft. Neue Forschungen im Umkreis der Glocknergruppe. *Wiss. Alpenvereinsh.* 21, 253–264.

Cantón, Y., Chamizo, S., Rodriguez-Caballero, E., Lázaro, R., Roncero-Ramos, B., RománSolé-Benet, J. R. A., et al. (2020). Water Regulation in Cyanobacterial Biocrusts from Drylands: Negative Impacts of Anthropogenic Disturbance. *Water* 12, 720. doi:10.3390/w12030720

Ciccazzo, S., Esposito, A., Borruso, L., and Brusetti, L. (2005). Microbial Communities and Primary Succession in High Altitude Mountain Environments. *Ann. Microbiol.* 66, 43. doi:10.1007/s13213-015-1130-1

Coen, M. C., Weingartner, E., Schaub, D., Hueglin, C., Corrigan, C., Schwikowski, M., et al. (2003). Saharan Dust Events at the Jungfraujoch: Detection by Wavelength Dependence of the Single Scattering Albedo and Analysis of the Events during the Years 2001 and 2002. *Atmos. Chem. Phys. Discuss.* 3, 5547–5594.

Di Mauro, B., Garzonio, R., Rossini, M., Filippa, G., Pogliotti, P., Galvagno, M., et al. (2019). Saharan Dust Events in the European Alps: Role in Snowmelt and Geochemical Characterization. *Cryosphere* 13, 1147–1165. doi:10.5194/tc-13-1147-2019

Dong, Z., Qin, D., Kang, S., RenChen, J. J., Chen, J., Cui, X., et al. (2014). Physicochemical Characteristics and Sources of Atmospheric Dust Deposition in Snow Packs on the Glaciers of Western Qilian Mountains, China. *Tellus B Chem. Phys. Meteorology* 66, 20956. doi:10.3402/tellusb.v66.20956

Duffy, L. (2011). *Mikroreliefbedingte Raummuster von Böden, äolischen Substraten und Flugstäuben im Hochgebirgskarst der Nördlichen Kalkalpen (Reiteralpe, Berchtesgadener Alpen). Doctoral thesis.* München: Ludwig Maximilian-Universität München, 131.

Eiby, G. A. (1959). A Survey of the Tektite Problem, *N. Z. J. Geol. Geophys.* 2, 183–194. doi:10.1080/00288306.1959.10431321

Ernstson, K., Hiltl, M., and Neumair, A. (2014). "Microtektite-like Glasses from the Northern Calcareous Alps (Southeast Germany): Evidence of a Proximal Impact Ejecta Origin," in 45th Lunar and Planetary Science Conference.

Evans, R. D., and Johansen, J. R. (1999). Microbiotic Crusts and Ecosystem Processes. *Crit. Rev. Plant Sci.* 18, 183–225. doi:10.1080/07352689991309199

Farmer, A. M. (1993). The Effects of Dust on Vegetation-A Review. *Environ. Pollut.* 79:1, 63–75. doi:10.1016/0269-7491(93)90179-r

Faul, H. (1966). Tektites Are Terrestrial. *Science* 152, 1341–1345. doi:10.1126/science.152.3727.1341

Fehr, K. T., Pohl, J., Mayer, W., Hochleitner, R., Fassbinder, J., Geiss, E., et al. (2005). A Meteorite Impact Crater Field in Eastern Bavaria? A Preliminary Report. *Meteor. Plan. Sci.* 40, 187–194. doi:10.1111/j.1945-5100.2005.tb00374.x

Fink, M. H. (1984). *Das Karstgebiet Beim Hochtor (Hohe Tauern, Salzburg-Kärnten).* Die Höhle *35*. Wien: Festschrift H. Trimmel, 127–134.

Folco, L., and Cordier, C. (2015). Micrometeorites. *EMU Notes Mineralogy* 155 (9), 253–297. doi:10.1180/EMU-notes.15.9

Franchy, G., Ojeda, A., López-Cancio, J., and Hernández-León, S. (2013). Plankton Community Response to Saharan Dust Fertilization in Subtropical Waters off the Canary Islands. *Biogeosci. Discuss.* 10, 17275–17307. doi:10.5194/bgd-10-17275-2013

Frank, W. (1969). Geologie der Glocknergruppe. *Wiss. AV-Hefte* 21, 5–114. doi:10.2118/2191-pa

French, B. M., and Koeberl, C. (2010). The Convincing Identification of Terrestrial Meteorite Impact Structures: What Works, what Doesn't, and Why. *Earth-Science Rev.* 98, 123–170. doi:10.1016/j.earscirev.2009.10.009

Friedel, H. (1936). Ein bodenkundlicher Ausflug in die Sandsteppe der Gamsgrube. *Mitt. Dt. Österr. Av.* 9, 220–222.

Ganapathy, R. (1983). The Tunguska Explosion of 1908: Discovery of Meteoritic Debris Near the Explosion Site and at the South Pole. *Science* 220, 1158–1161. doi:10.1126/science.220.4602.1158

Genge, M. J., Engrand, C., Gounelle, M., and Taylor, S. (2008). The Classification of Micrometeorites. *Met. Planet. Sci.* 43, 497–515. doi:10.1111/j.1945-5100.2008.tb00668.x

Gild, C., Geitner, C., and Sanders, D. (2018). Discovery of a Landscape-wide Drape of Late-Glacial Aeolian Silt in the Western Northern Calcareous Alps (Austria): First Results and Implications. *Geomorphology* 301, 39–52. doi:10.1016/j.geomorph.2017.10.025

Glass, B. P. (1990). Tektites and Microtektites: Key Facts and Inferences. *Tectonophysics* 171 (1– 4), 393–404. doi:10.1016/0040-1951(90)90112-L

Goudie, A. S., and Middleton, N. J. (2006). *Desert Dust in the Global System*. Springer, 287.

Gračanin, Z. (1972). Vertikale und horizontale Verteilung der Bodenbildung auf Kalken und Dolomiten im mittleren Abschnitt der Alpen. *Mitt. Dt. Bodenkd. Ges.* 15, 19–40.

Grashey-Jansen, S., Korch, O., Beck, C., Friedmann, A., Bernhard, R., and Dubitzky, C. (2014). Aeolian Influenced Soil Sites in Consideration of Atmospheric Circulation Types – a Case Study in the Alpine Zone of the Zugspitzplatt (Northern Calcareous Alps, Germany). *Int. J. Geol. Agric. Environ. Sci.* 2:4, 11–19.

Greilinger, M., Schauer, G., Baumann-Stanzer, K., SkomorowskiSchöner, P. W., Schöner, W., and Kasper-Giebl, A. (2018). Contribution of Saharan Dust to Ion Deposition Loads of High Alpine Snow Packs in Austria (1987-2017). *Front. Earth Sci.* 6. doi:10.3389/feart.2018.00126

Gruber, F. (1980). "Die Verstaubung der Hochgebirgsböden im Glocknergebiet," in *Untersuchungen an alpinen Böden in den Hohen Tauern 1974–1978, Stoffdynamik und Wasserhaushalt*. MaB-Hochgebirgsprogramms Hohe Tauern, *3*. Österr. Akad. Wiss. Editors H. Franz and V. Österr (Wagner, Innsbruck, 69–91.

Guerzoni, S., Molinaroli, E., and Chester, R. (1997). Saharan Dust Inputs to the Western Mediterranean Sea: Depositional Patterns, Geochemistry and Sedimentological Implications: *Deep Sea Res. Part II Top. Stud. Oceanogr.* 44, 631–654. doi:10.1016/s0967-0645(96)00096-3

Haeberli, W. (1978). Sahara Dust on the Alps - A Short Review. *Z. Gletscherk. Glazialgeol.* 13, 206–208.

Höck, V. (1980). Distribution Maps of Minerals of the Alpine Metamorphism in the Penninic Tauern Window, Austria. *Mitt, Österr. Gol. Ges.* 71/72, 119–127.

Huber, K., Peer, T., Tschaikner, A., Türk, R., and Guber, J. P. (2007). *Characteristics and Function of Soil Crusts in Different Successional Stages in Alpine Environments, Outlined on an Alpine Lime Scree in the Großglockner Region (Austria)*, 74. Wien: Mitt. Bodkdl. Ges., 111–126.

Jahn, R. (2010). "Impact of Aeolian Sediments on Pedogenesis – Examples from the Fringe Area of the Saharan Desert," in 19th World Congress of Soil Science, Soil Solutions for a Changing World, Brisbane, Australia, 1 – 6 August 2010.

Johnston, S. W. (2001). The Influence of Aeolian Dust Deposits on Alpine Soils in South-Eastern Australia. *Soil Res.* 39, 81–88. doi:10.1071/SR99121

Jung, P., Baumann, K., Emrich, D., Springer, A., Felde, V. J. M. N. L., Dultz, S., et al. (2020). Lichens Bite the Dust - A Bioweathering Scenario in the Atacama Desert. *iScience* 23, 101647. doi:10.1016/j.isci.2020.101647

Kalińska-Nartiša, E., Lamsters, K., Karušs, J., Krievāns, M., Rečs, A., and Meija, R. (2017). Quartz Grain Features in Modern Glacial and Proglacial Environments: A Microscopic Study from the Russell Glacier, Southwest Greenland. *Pol. Polar Res.* 38, 265–289. doi:10.1515/popore-2017-0018

Kanakidou, M., Myriokefalitakis, S., and Tsigaridis, K. (2018). Aerosols in Atmospheric Chemistry and Biogeochemical Cycles of Nutrients. *Environ. Res. Lett.* 13, 063004. doi:10.1088/1748-9326/aabcdb

Kellogg, C. A., and Griffin, D. W. (2006). Aerobiology and the Global Transport of Desert Dust. *Trends Ecol. Evol.* 21, 638–644. doi:10.1016/j.tree.2006.07.004

King, E. A. (2020). The Origin of Tektites. A Brief Review. *Am. Sci.* 65, 212–218.

Kinzel, H. (1983). "Influence of Limestone, Silicates and Soil pH on Vegetation", in *Physiological Plant Ecology III. Encyclopedia of Plant Physiology (New Series)*, *12*, eds. O. L. Lange, P. S. Nobel, and V. B. Osmond, and Springer, Berlin, Heidelberg: H. Ziegler, 201–244. doi:10.1007/978-3-642-68153-0_7

Koeberl, C. (1990). The Geochemistry of Tektites: An Overview. *Tectonophysics* 171 (1– 4), 405–422. doi:10.1016/0040-1951(90)90113-M

Koeberl, C. (1994). Tektites Origin by Hypervelocity Asteroidal or Cometary Impact: Target Rocks, Source Craters, and Mechanisms. *Geol. Soc. Am. Spec. Pap.* 293, 133–151.

Körner, C. (1995). "Alpine Plant Diversity: A Global Survey and Functional Interpretations", in *Arctic and Alpine Biodiversity: Patterns, Causes and Ecosystem Consequences*, eds. F. S. Chapin, III, and Springer, Berlin, Heidelberg: Ch. Körner, 45–63. doi:10.1007/978-3-642-78966-3_FM

Krinsely, D. H., Friend, P. F., and Klimentidis, R. (1976). Eolian Transport Textures on the Surfaces of Sand Grains of Early Triassic Age. *GSA Bull.* 87 (1), 130–132. doi:10.1130/0016-7606(1976)87<130:ETTOTS>2.0.CO;2

Küfmann, C. (2003). Soil Types and Aeolian Dust in High Mountainous Karst of the Northern Calcareous Alps. (Zugspitzplatt, Wetterstein Mountains, Germany). *Catena* 53, 211–227. doi:10.1016/S0341-8162(03)00075-4

Küfmann, C. (2008a). Are Cambisols in Alpine Karst Autochthonous or Eolian in Origin? *Arc. Antarc. Alp. Res.* 40, 506–518.

Küfmann, C. (2008b). Flugstaubeintrag und Bodenbildung im Karst der Nördlichen Kalkalpen. . *Natl. Berchtesgad. Forschungsbericht* 54, 189.

Kutchko, B., and Kim, A. (2006). Fly Ash Characterization by SEM-EDS–EDS. *Fuel* 85, 2537–2544. doi:10.1016/j.fuel.2006.05.016

Letsch, D. (2014). The Distinction between Carbonate Cement and Internal Sediment in Quaternary Gravels: A Combined Field, Petrographic, and Stable Isotope Study from Northern Switzerland. *Esr* 3, 56–71. doi:10.5539/esr.v3n1p56

Lin, Y.-C., and Feng, J.-L. (2015). Aeolian Dust Contribution to the Formation of Alpine Soils at Amdo (Northern Tibetan Plateau). *Geoderma* 259-260, 104–115. doi:10.1016/j.geoderma.2015.05.012

Love, S. G., and Brownlee, D. E. (1993). A Direct Measurement of the Terrestrial Mass Accretion Rate of Cosmic Dust. *Science* 262, 550–553. doi:10.1126/science.262.5133.550

Lowman, P. D. (1962). Tektites vs. Terrestrial Rocks: a Comparison of Variance in Compositions. *Geochimica Cosmochimica Acta* 26, 561–579. doi:10.1016/0016-7037(62)90105-9

Loÿe-Pilot, M. D., Martin, J. M., and Morelli, J. (1986). Influence of Saharan Dust on the Rain Acidity and Atmospheric Input to the Mediterranean. *Nature* 321, 427–428. doi:10.1038/321427a0

Maestre, F. T., Bowker, M. A., Eldridge, D. J., Cortina, J., Lázaro, R., Gallardo, A., et al. (2016). "Biological Soil Crusts as a Model System in Ecology", in *Biological Soil Crusts: An Organizing Principle in Drylands*, eds. B. Weber, B. Büdel, and J. Belnap. *Ecological Studies (Analysis and Synthesis)* 226, 407–425. doi:10.1007/978-3-319-30214-0_20

Mahaney, W. C., Somelar, P., West, A., Krinsley, D., Allen, C. C. R., Pentlavalli, P., et al. (2017). Evidence for Cosmic Airburst in the Western Alps Archived in Late Glacial Paleosols. *Quat. Int.* 438, 68–80. doi:10.1016/j.quaint.2017.01.043

Maki, T., Lee, K. C., Kawai, K., Onishi, K., Hong, C. S., Kurosaki, Y., et al. (2019). Aeolian Dispersal of Bacteria Associated with Desert Dust and Anthropogenic Particles over Continental and Oceanic Surfaces. *J. Geophys. Res. Atmos.* 124, 5579–5588. doi:10.1029/2018JD029597

Maupetit, F., and Delmas, R. J. (1994). Snow Chemistry of High Altitude Glaciers in the French Alps. *Tellus B Chem. Phys. Meteorology* 46, 304–324. doi:10.3402/tellusb.v46i4.15806

Meola, M., Lazzaro, A., and Zeyer, J. (2015). Bacterial Composition and Survival on Sahara Dust Particles Transported to the European Alps. *Front. Microbiol.* 6, 1454. doi:10.3389/fmicb.2015.01454

Middleton, N., and Goudie, A. (2002). Saharan Dust: Sources and Trajectories. *Earth Sci. Rev.* 56:1– 4, 179–204. doi:10.1016/S0012-8252(01)00067-8

Mix, C., and Küfmann, C. (2015). Sedimenttransport zwischen Dolinenkarst und Riesendinghöhle am Untersberg (Nördliche Kalkalpen). *zfg.* 59, 455–475. doi:10.1127/zfg/2015/0165

Mladenov, N., Williams, M. W., Schmidt, S. K., and Cawley, K. (2012). Atmospheric Deposition as a Source of Carbon and Nutrients to Barren, Alpine Soils of the Colorado Rocky Mountains. *Biogeosci. Discuss.* 9, 2375–2424. doi:10.5194/bgd-9-2375-2012

Muhs, D. R., and Benedict, J. B. (2006). Eolian Additions to Late Quaternary Alpine Soils, Indian Peaks Wilderness Area, Colorado Front Range. *Arct. Antarct. Alp. Res.* 38, 120–130. doi:10.1657/1523-0430(2006)038[0120:eatlqa]2.0.co;2

Muhs, D. R., Prospero, J. M., Baddock, M. C., and Gill, T. E. (2014). "Identifying Sources of Aeolian Mineral Dust: Present and Past," in *Identifying Sources of Aeolian Mineral Dust: Present and Past" in Mineral Dust: A Key Player in the Earth System*. Editors J. B. Stuut and P. Knippertz, 51–74. doi:10.1007/978-94-017-8978-3_3

Newsome, D., and Ladd, P. (1999). The Use of Quartz Grain Microtextures in the Study of the Origin of Sand Terrains in Western Australia. *Catena* 35, 1–17. doi:10.1016/S0341-8162(98)00122-2

O'Keefe, J. A. (1966). The Origin of Tektites. *Space Sci. Rev.* 6, 174–221. doi:10.1007/bf00222593

Okin, G. S., Mahowald, N., Chadwick, O. A., and Artaxo, P. (2004). Impact of Desert Dust on the Biogeochemistry of Phosphorus in Terrestrial Ecosystems. *Glob. Biogeochem. Cycles* 18, a–n. doi:10.1029/2003GB002145

Peer, T., Neubauer, R., and Friedl, G. (2021). *Das Hochtor, ein internationales Forschungsgebiet für biologische Bodenkrusten und weiterführende Untersuchungen*. Klagenfurt:Carinthia II 211/131, 81–98.

Peer, T., Türk, R., Gruber, J. P., and Tschaikner, A. (2010). Species Composition and Pedological Characteristics of Biological Soil Crusts in a High Alpine Ecosystem, Hohe Tauern, Austria. *ecomont* 2, 23–30. doi:10.1553/eco.mont-2-1s23

Prasad, M. S., Rudraswami, N. G., and Panda, D. K. (2013). Micrometeorite Flux on Earth during the Last ~50,000 Years. *J. Geophys. Res. Planets* 118, 2381–2399. doi:10.1002/2013JE004460

Prodi, F., and Fea, G. (1978). Transport and Deposition of Saharan Dust over Alps. *Proc. 15th Intern. Meet. Alp. Meteorol., Grindelwald 19– 23 Sept.* 1, 179–182.

Ramanathan, V., and Carmichael, G. (2008). Global and Regional Climate Changes Due to Black Carbon. *Nat. Geosci.* 1 (4), 221–227. doi:10.1038/ngeo156

Ramdohr, P. (1969). *The Ore Minerals and Their Intergrowths*. International Series of Monographs on Earth Sciences. Oxford New York: Pergamon Press, 1174.

Rapp, A. (1983). Are Terra Rossa Soils in Europe Eolian Deposits from Africa? *Geol. Föreningen i Stockh. Förhandlingar.* 105(2), 161–168. doi:10.1080/11035898309454562

Rappenglück, M. A., Rappenglück, B., and Ernstson, K. (2017). Cosmic Collision in Prehistory –The Chiemgau Impact: Research in a Bavarian Meteorite Crater Strewn Field. *Zs. Anomalistik* 17, 235– 260.

Reitbauer, V. (2010). *Zum calcicolen-calcifugen Komplex. Das Vorkommen "acidophiler" Gefäßpflanzen auf Karbonatböden im Glocknergebiet*. Master thesis. Salzburg: University of Salzburg, 105.

Rime, T., Hartmann, M., and Frey, B. (2016). Potential Sources of Microbial Colonizers in an Initial Soil Ecosystem after Retreat of an Alpine Glacier. *ISME J.* 10, 1625–1641. doi:10.1038/ismej.2015.238

Rizzolo, J. A., Barbosa, C. G. G., Borillo, G. C., Godoi, A. F. L., Souza, R. A. F., Andreoli, R. V., et al. (2016). Mineral Nutrients in Saharan Dust and Their Potential Impact on Amazon Rainforest Ecology. *Atmos. Chem. Phys. Discuss.* doi:10.5194/acp-2016-557

Rossi, F., Li, H., Liu, Y., and De Philippis, R. (2017). Cyanobacterial Inoculation (Cyanobacterisation): Perspectives for the Development of a Standardized Multifunctional Technology for Soil Fertilization and Desertification Reversal. *Earth-Science Rev.,* 171, 28–43. doi:10.1016/j.earscirev.2017.05.006

Rozenstein, O., Zaady, E., Katra, I., Karnieli, A., Adamowski, J., and Yizhaq, H. (2014). The Effect of Sand Grain Size on the Development of Cyanobacterial Biocrusts. *Aeolian Res.* 15, 217–226. doi:10.1016/j.aeolia.2014.08.003

Schauer, G., Kasper-Giebl, A., and Močnik, G. (2016). Increased PM Concentrations during a Combined Wildfire and Saharan Dust Event Observed at High-Altitude Sonnblick Observatory, Austria. *Aerosol Air Qual. Res.* 16, 542–554. doi:10.4209/aaqr.2015.05.0337

Schmid, S. M., Scharf, A., Handy, M. R., and Rosenberg, C. L. (2013). The Tauern Window (Eastern Alps, Austria): A New Tectonic Map, with Cross-Sections and a Tectonometamorphic Synthesis. *Swiss J. Geosci.* 106, 1–32. doi:10.1007/s00015-013-0123-y

Schmidt, S. K., Reed, S. C., Nemergut, D. R., Stuart Grandy, A., Cleveland, C. C., Weintraub, M. N., et al. (2008). The Earliest Stages of Ecosystem Succession in High-Elevation (5000 Metres above Sea Level), Recently Deglaciated Soils. *Proc. R. Soc. B* 275 (1653), 2793–2802. doi:10.1098/rspb.2008.0808

Schüssler, U., Rappenglück, M. A., Ernstson, K., Mayer, W., and Rappenglück, B. (2005). Das Impakt-Krater-Streufeld im Chiemgau. *Euro. J. Mineral.* 17 (1), 124.

Schwikowsky, M., Seibert, P., Baltensperger, U., and Gäggeler, H. W. (1995). A Study of an Outstanding Saharan Dust Event at the High-Alpine Site Jungfraujoch, Switzerland. *Atmos. Environ.* 29, 1829– 1842.

Sharma, S. B., Sayyed, R. Z., Trivedi, M. H., and Gobi, T. A. (2013). Phosphate Solubilizing Microbes: Sustainable Approach for Managing Phosphorus Deficiency in Agricultural Soils. *Springerplus* 2, 587–600. doi:10.1186/2193-1801-2-587

Simonson, R. W. (1995). Airborne Dust and its Significance to Soils. *Geoderma* 65, 1– 43. doi:10.1016/0016-7061(94)00031-5

Sodemann, H., Palmer, A. S., Schwierz, C., Schwikowski, M., and Wernli, H. (2005). The Transport History of Two Saharan Dust Events Archived in an Alpine Ice Core. *Atmos. Chem. Phys. Discuss.* 5, 7497–7545. Avaliable at: www.atmos-chem-phys.org/acpd/5/7497/.

Solar, F. (1964). Zur Kenntnis der Böden auf dem Raxplateau. *Mitt. Österr. Bodenk. Ges.* 8, 72.

Sticher, H., Bach, R., Brugger, H., and Vökt, U. (1975). Flugstaub in Vier Böden Aus Kalk, Dolomit Und Serpentin (Schweizer Jura Und Schweizer Alpen). *Catena* 2, 11–22. doi:10.1016/S0341-8162(75)80002-6

Stuut, J.-B., Smalley, I., and O'Hara-Dhand, K. (2009). Aeolian Dust in Europe: African Sources and European Deposits. *Quat. Int.*198, 234–245. doi:10.1016/j.quaint.2008.10.007

Taylor, S., Messenger, S., and Folco, L. (2016). Cosmic Dust: Finding a Needle in a Haystack. *Elements* 12, 171–176. doi:10.2113/gselements.12.3.171

Telloli, C., Chicca, M., Pepi, S., and Vaccaro, C. (2018). Saharan Dust Particles in Snow Samples of Alps and Apennines during an Exceptional Event of Transboundary Air Pollution. *Environ. Monit. Assess.* 190, 37. doi:10.1007/s10661-017-6412-6

Tomadin, L., Wagenbach, D., and Landuzzi, V. (1996). "Mineralogy and Source of High Altitude Glacial Deposits in the Western Alps: Clay Minerals as Saharan Dust Tracers", in *The Impact of Desert Dust across the Mediterranean*, eds. S. Guerzoni and R. Chester, 223– 232.doi:10.1007/978-94-017-3354-0_22

Van-Soest, M. (2021). *Modern Aeolian Dust Deposition on Arctic Soils in South West Greenland: Linkages between Geomorphology and Ecosystem Dynamics in Space and Time*. dissertation. Loughborough, United Kingdom: Loughborough University. doi:10.26174/thesis.lboro.13553921.v1

Varga, G., Cserháti, C., Kovács, J., and Szalai, Z. (2016). Saharan Dust Deposition in the Carpathian Basin and its Possible Effects on Interglacial Soil Formation. *Aeolian Res.* 22, 1– 12. doi:10.1016/j.aeolia.2016.05.004

Vinšová, P., Luláková, P., Čapek, P., Falteisek, L., Yde, J., Skoblia, S., et al. (2018). "Soil Development on a High Arctic Glacier Forefield: How Is the Microbial Community Limited by Nutrient Availability? 20th EGU General Assembly, EGU2018," in Proceedings from the conference held 4-13 April, 2018 Vienna, Austria, 17150.

Wagenbach, D., and Geis, K. (1989). "The Mineral Dust Record in a High Altitude Alpine Glacier (Colle Gnifetti, Swiss Alps)," in *Paleoclimatology and Paleometeorology: Modern and Past Patterns of Global Atmospheric Transport. NATO ASI Series (Series C: Mathematical and Physical Sciences)*. Editors M. Leinen and M. Sarnthein, 282, 543–564. 978-94-009-0995-3. doi:10.1007/978-94-009-0995-3_23

Wagenbach, D., Preunkert, S., Schäfer, J., Jung, W., and Tomadin, L. (1996). "Northward Transport of Saharan Dust Recorded in a Deep Alpine Ice Core," in *The Impact of Desert Dust a Cross the Mediterranean*. Editors S. Guerzoni and T. Chester (Dortrecht, Netherlands: Kluwer Academic Publishers), 291–300. doi:10.1007/978-94-017-3354-0_29

Warren, S. D., Clair, L. L., and Leavitt, S. D. (2019). Aerobiology and Passive Restoration of Biological Soil Crusts. *Aerobiologia* 35, 5. doi:10.1007/s10453-018-9539-1

Weber, B., Büdel, B., and Belnap, J. (Editors) (2003). "Biological Soil Crusts: An Organizing Principle in Drylands," *Ecological Studies*, 226.

Weber, B., Bowker, M., Zhang, Y., and Belnap, J. (2016). "Natural Recovery of Biological Soil Crusts after Disturbance," in *Biological Soil Crusts: An Organizing Principle in Drylands. Ecological Studies (Analysis and Synthesis)*, eds. B. Weber, B. Büdel, and J. Belnap, 479–498. doi:10.1007/978-3-319-30214-0_23

Williams, L., Jung, P., Zheng, L.-J., Maier, S., Peer, T., Grube, M., et al. (2017). Assessing Recovery of Biological Soil Crusts across a Latitudinal Gradient in Western Europe. *Restor. Ecol.* 26, 543–554. doi:10.1111/rec.12579

Williams, L., Loewen-Schneider, K., Maier, S., and Büdel, B. (2016). Cyanobacterial Diversity of Western European Biological Soil Crusts along a Latitudinal Gradient. *FEMS Microbiol. Ecol.* 92, fiw157. doi:10.1093/femsec/fiw157

Wohlgemuth, T., and Gigon, A. (2003). Calcicole Plant Diversity in Switzerland May Reflect a Variety of Habitat Templets. *Folia Geobot.* 38, 443–452. doi:10.1007/BF02803251

Woronko, B., Zieliński, P., and Sokołowski, R. J. (2015). Climate Evolution during the Pleniglacial and Late Glacial as Recorded in Quartz Grain Morphoscopy of Fluvial to Aeolian Successions of the European Sand Beltfluvial to Aeolian Successions of the European Sand Belt. *Geologos* 21, 89–103. doi:10.1515/logos-2015-0005

Yaalon, D. H., and Ganor, E. (1973). The Influence of Dust on Soils during the Quaternary. *Soil Sci.*116, 146–155. doi:10.1097/00010694-197309000-00003

Yan, Y., Xu, X., Xin, X., Yang, G., Wang, X., Yan, R., et al. (2011). Effect of Vegetation Coverage on Aeolian Dust Accumulation in a Semiarid Steppe of Northern China. *Catena* 87, 351–356. doi:10.1016/j.catena.2011.07.002

Yang, H., Liu, L., Li, X., WeiLi, Y. X., Li, X., and Jia, R. (2014). Water Repellency of Biological Soil Crusts and Influencing Factors on the Southeast Fringe of the Tengger Desert, North-Central China. *Soil Sci.* 179 (9), 424–432. doi:10.1097/ss.0000000000000084

Yoshitake, S., Uchida, M., Koizumi, H., and Nakatsubo, T. (2007). Carbon and Nitrogen Limitation of Soil Microbial Respiration in a High Arctic Successional Glacier Foreland Near Ny-Ålesund, Svalbard. *Polar Res.* 26, 22–30. doi:10.1111/j.1751-8369.2007.00001.x

Żbik, M. (1984). Morphology of the Outermost Shells of the Tunguska Black Magnetic Spherules. *J. Geophys. Res.* 89, B605–B611. doi:10.1029/JB089iS02p0B605

Zemp, M., Haeberli, W., Hoelzle, M., and Paul, F. (2006). Alpine Glaciers to Disappear within Decades? *Geophys. Res. Lett.* 33. doi:10.1029/2006GL026319

Zheng, L. J., Mair, S., Grube, M., Türk, R., Gruber, J. P., and Peer, T. (2014). Alpine Biological Soil Crusts on the Hochtor (Grossglockner High Alpine Route, Hohe Tauern, Austria): Soils, Function and Biodiversity. *Acta zoobot. Austria* 150/151, 175–196.

Zierold, K. M., and Odoh, C. (2020). A Review on Fly Ash from Coal-Fired Power Plants: Chemical Composition, Regulations, and Health Evidence. *Rev. Environ. Health* 35 (4), 401–418. doi:10.1515/reveh-2019-0039